

POLITECNICO DI TORINO

**MASTER OF SCIENCE IN MECHATRONIC
ENGINEERING**



Master's Degree Thesis

**Innovative Concept for Robust Control of
exhaust valves application**

Supervisors

Prof. GIOVANNI BRACCO

Co-Sup. FRANCESCO NIOSI

Candidate

GIANMARIA GIARDINA

JULY 2023

Abstract

In this thesis project a robust control for an electronic throttle valve(ETV) is developed. The thesis is held in collaboration with the company **Testing Technologies s.r.l.**

The designed controller is intended to be used for testing purposes by exploiting the testbench of the company, in particular the aim is to have a controller able to adapt to different valve models and so to be independent from the parameters of the valve itself in order to speed up the testing procedure and to avoid the re-characterization of the model for every valve. After an introduction and overview on the state-of-the-art, the mathematical model of the valve is presented. Then three types of controllers have been examined. Starting from the work previously done for the company, a controller based on Youla-Coucera parametrization and a Feedforward compensation is taken in exam, then a more performing and robust controller is designed based on Sliding Mode Control techniques. First developing a classical Sliding Mode controller(SMC) and then exploiting the Higher order Sliding modes theory(HOSM) to realize a Super Twisting Sliding Mode Controller(STSMC).The classical SMC is more robust with respect to the Youla-Coucera controller, but has still some dependence on the valve parameters in the computation of the sliding surface. Instead the STSMC configuration is independent from the parameters of the valve, and for the design only bounds on the second derivative of the sliding surface are needed, making it suitable for a trial and error procedure and for self tuning.

The control algorithms are implemented in Simulink for simulation purposes, then an equivalent scheme on labview has to be developed to integrate the controller in the testbench. To conclude, the three controllers have been compared considering the performances and the intrinsic predisposition to be easily tuned and the independence on ETV parameters.

Acknowledgements

Table of Contents

List of Tables	VII
List of Figures	VIII
1 Introduction	1
1.1 Project overview	1
1.2 Electronic Throttle Control	2
1.3 State of the art	3
2 Case study	5
2.1 ETV model	5
2.1.1 DC motor model expression	6
2.1.2 Static characteristic	6
2.1.3 Dynamic characteristic	7
2.1.4 Parameter tables	8
2.2 Simulink model	9
2.2.1 Frequency response	11
3 Control techniques	13
3.1 Youla-Coucera parametrization and FF compensation	13
3.1.1 Youla-Coucera parametrization	13
3.1.2 Plant inversion and shaping filter	14
3.1.3 Feedforward compensation	15
3.2 Sliding mode control	16
3.2.1 General Framework	18
3.2.2 Choice of the sliding surface	19
3.2.3 Control action formulation	19
3.2.4 Chattering compensation	20
3.3 Super Twisting sliding mode algorithm	21
3.3.1 Super Twisting Algorithm	21

4	Numerical implementation	23
4.1	Sliding Mode implementation	23
4.1.1	Integration problems	25
4.2	STSMC implementation	25
4.2.1	Simulink scheme functional description	25
4.2.2	Step simulations	27
4.2.3	Stair signal simulation	28
4.2.4	Sine wave simulations	30
4.2.5	Triangular wave simulation	31
5	Simulation tests and comparisons	33
5.1	Testbench characteristics	33
5.2	labVIEW implementation of Youla-Coucera configuration	35
5.3	Step response comparison	35
5.4	Stair response comparison	37
5.5	Sine response comparison	37
5.6	Final considerations	38
6	Conclusions	42
6.1	Future works	43
A	MATLAB code	44
A.1	Sliding Mode Controller nonlinear term evaluation	44
A.2	Sliding Mode Controller implementation	44
A.3	Super Twisting SMC implementation	45
B	labVIEW code	46
	Acronyms	47
	Bibliography	48

List of Tables

2.1	Motor section parameters	8
2.2	ETV static parameters	9
2.3	Loss parameters and Dynamic parameters	9
4.1	Settling times of STSMC	28

List of Figures

1.1	General ETV control setup [3]	2
1.2	General closed loop control scheme	3
2.1	General ETV scheme [8]	5
2.2	Valve static characteristic[4]	7
2.3	Block scheme of the ETV model used in the thesis	8
2.4	Simulink model of DC motor	10
2.5	Rotor mechanical equilibrium block	10
2.6	Full simulink scheme of the ETV model	11
2.7	Full simulink scheme of the ETV model	12
3.1	Closed loop scheme	13
3.2	Feed Forward scheme	15
3.3	Phase trajectory of system 3.11 using control law 3.13	17
3.4	Chattering visualization	18
4.1	Simulink implementation of SMC	25
4.2	Simulink implementation of STSMC	26
4.3	Descriptive scheme for 4.2	26
4.4	Step response of STSMC	27
4.5	Zoom of the signal and set angle of 80° at steady state	29
4.6	Step response for various small angle set	29
4.7	Stair signal simulation	30
4.8	Stair signal simulation error	30
4.9	Simulation with a sinewave at 5rad frequency	31
4.10	Triangular wave simulation	32
5.1	Testbench scheme	34
5.2	labVIEW representation of Feed Forward control action	35
5.3	labVIEW representation of closed loop control action	36
5.4	Step response comparison for 60 degree angle	36
5.5	Settling time comparison	37

5.6	Steady state error using Youla-Coucera controller	38
5.7	Step simulation for Youla-Coucera system	39
5.8	Stair simulation comparison	39
5.9	Stair simulation error of Youla-Coucera	40
5.10	Sine Simulation Comparison	40
5.11	Sine Simulation at 1Hz (Youla-Coucera)	41
B.1	Evaluation of nonlinear actions in labVIEW	46

Chapter 1

Introduction

1.1 Project overview

In internal combustion engines the throttle valve is responsible of the air intake in the combustion chamber. The position of the valve affects the performances of the engine and other aspects such as[1]:

- Idle control
- Speed control
- Fuel consumption
- Emissions

Due to the stringent constraints on emissions for environmental reasons and optimization of safety and performance, the improvement of the aspects mentioned above is necessary, and so a good control design is essential to achieve such objective. The position of the plate of the valve is controlled in two ways:

- Mechanical control
- Electronic control or Drive by wire

In the first case the throttle plate position is mechanically connected to the gas pedal. In this way when the pedal is pushed the mechanical rod pulls the spring and opens the valve depending on the position of the pedal.

In ETVs the position of the pedal is measured by sensors, this information is sent to the ECU that elaborates the optimal valve's plate position. This solution is called drive by wire because isn't directly connected by a mechanical system but is driven from distance by an electronic wire that enable the movement by a DC motor[2].

1.2 Electronic Throttle Control

The control of an ETV is an important aspect in modern automotive technologies. As for other components the optimization of such control is needed, other than the safety and emission optimization mentioned in the previous section, for the improvement of autonomous driving technologies. The information taken in account to evaluate the optimal control action does not depend strictly on the only pedal position but also on other sensor data:

- Speed sensor
- Pre-collision system sensors
- Wheel speed sensor
- Air flow sensor

All the information brought by all the sensors are used by the by the Electronic Control Unit (or Electronic Control Module) in order to evaluate the optimal valve position set angle.

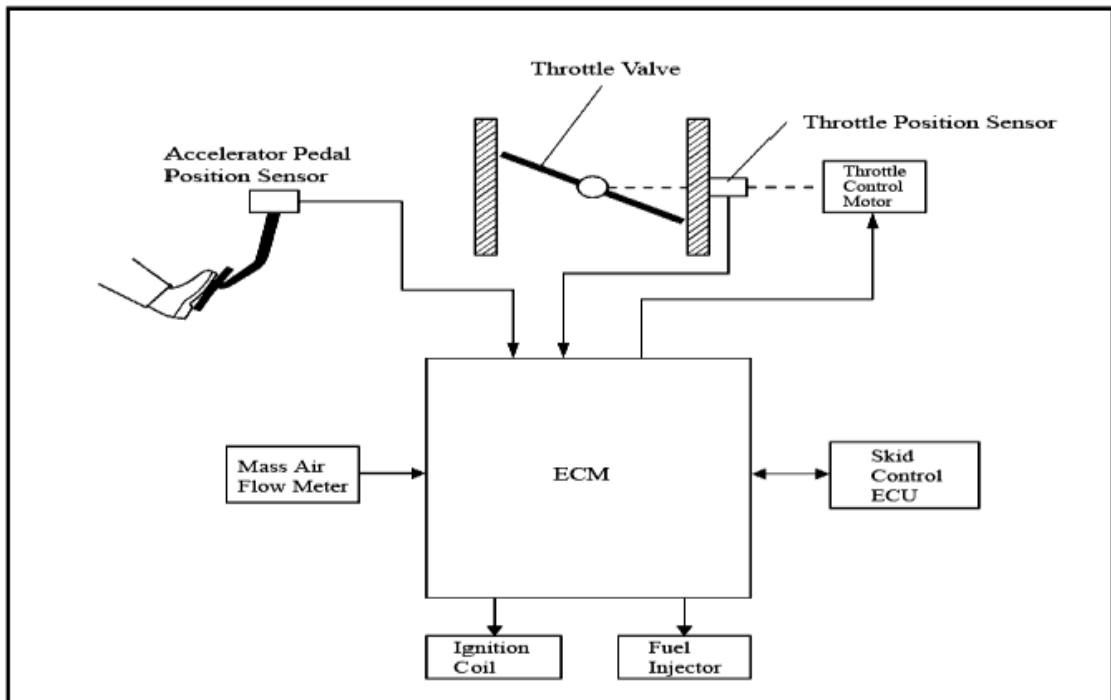


Figure 1.1: General ETV control setup [3]

The general scheme of the control system is a closed loop system that take as feedback the informations about the actual position of the valve to adjust the control action effort to give to the system.

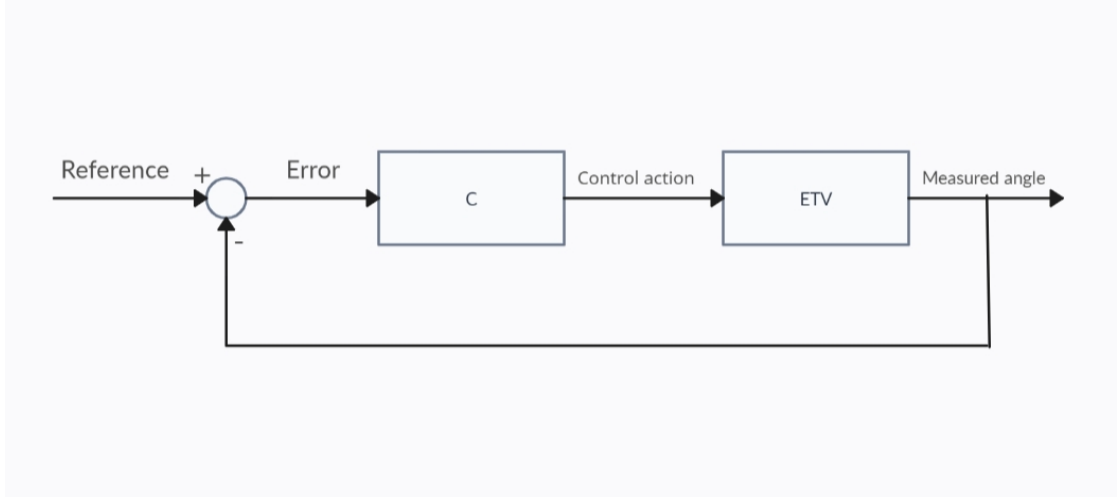


Figure 1.2: General closed loop control scheme

1.3 State of the art

In ETVs the main problem to overcome is given by the intrinsic strong non-linearities given by the return spring and the friction phenomenon in the plate and the other moving parts. Many solutions have been proposed in literature to compensate the non-linearity effects. In [4] a solution with Youla-coucera parametrization and feed-forward compensation of the non-linearities have been proposed. The controller is of simple design and the solution provide good tracking performances but is strongly dependent on the ETV parameters and so a recharacterization must be done if we want to use the same controller on a different valve.

A different kind of approach is to use directly a non-linear control technique like in [5], in which a VSS based controller have been used, exploiting a three level cascade controller that ensures robustness. This structure was chosen in order to make easier the physical implementation of the controller in terms of components and computational effort. The recent technological improvements, providing more powerful microcontrollers allows to use nonlinear techniques that are computationally more demanding than the previous structure proposed but of simpler implementation. To this purpose a controller based on SMC theory have been considered since it provides robustness to the uncertainties of the valve parameter but it is also dependent on them for the design of the sliding surface.

In [6] a controller based on HOSM theory have been proposed to overcome the problem of chattering typical of the classical SMC. The design of this kind of controller is dependant only on some constraint given on the parameters; these constraints are connected only to the bound of some uncertainty function, so is completely independent on the values of the ETV parameters. This characteristic allow the design of an Adaptive algorithm form the automatic tuning of the controller parameters, making this technique suitable to be used for different type of valves without the recharacterization of the parameters. A similar solution have been used in [7], exploiting the STSMC algorithm that provides all the advantages of the previous cited study but also a simpler practical implementation.

Chapter 2

Case study

2.1 ETV model

In order to develop a controller for the ETV a model of the system is needed.

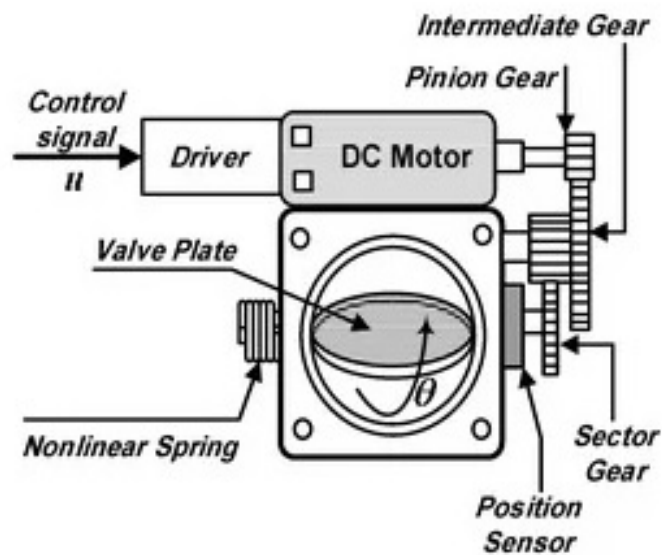


Figure 2.1: General ETV scheme [8]

The derived mathematical model of the valve has been obtained in [4] deriving the parameter values of the different parts of the system i.e. :

- DC motor
- Static and dynamic characteristic of the valve

2.1.1 DC motor model expression

The armature resistance and inductance has been obtained exploiting the blocked rotor test driving the armature with respectively a constant voltage and then a sinusoidal one. Then the electromotive force coefficient has been estimated connecting the motor to the valve and bringing the plate to 90° angle and letting it freely return to the resting position and calculating the voltage in open circuit. With all the calculated parameters it is possible to derive the mathematical expression of the DC motor section :

$$V_a = R_a i_a + L \frac{di_a(t)}{dt} + k_e \omega_m(t) \quad (2.1)$$

Were V_a is the armature voltage, R_a is the armature resistance, i_a is the armature current, k_e is the back EMF coefficient and ω_m is the speed of the rotor.

2.1.2 Static characteristic

In order to determine the static characteristic of the valve it is at first necessary to evaluate the total losses of the motor, that is the sum of the Joule losses and the losses due to friction, ventilation phenomenon and viscous friction.

$$P_{loss} = VI = R_a I^2 + P_0(\omega_m)$$

Where P_0 is equal to :

$$P_0(\omega_m) = (T_{cm} + B_m \omega_m + C_{dm} \omega_m^2) \omega_m \quad (2.2)$$

Given that T_{cm} is the Coulombian friction coefficient, B_m is the viscous friction coefficient and C_{dm} is the ventilation coefficient. The behavior of the valve in static condition is then described by the following expression:

$$T_u = (k_t i_a - P_0(\omega_m)) \tau = K_s (\theta - \theta_0) + T_{PL} + T_c \text{sign}(\dot{\theta}) \quad (2.3)$$

Where k_t is the motor torque coefficient, K_s is the spring coefficient, T_{PL} is the spring preload torque and T_c is the Coulombian friction torque. These coefficient are evaluated determining the characteristic of the valve during a full opening and closing of the valve done at constant velocity in order to consider negligible the equivalent inertia of the system. The results leads to a discontinuous characteristic caused by the nonlinear behavior of the spring and so two different value of the parameters ,depending on the position of the valve, are obtained.

From figure 2.2 is also possible to evaluate the resting angle θ_0 that is the angle that corresponds to the flat section of the characteristic(i.e. the discontinuity point).

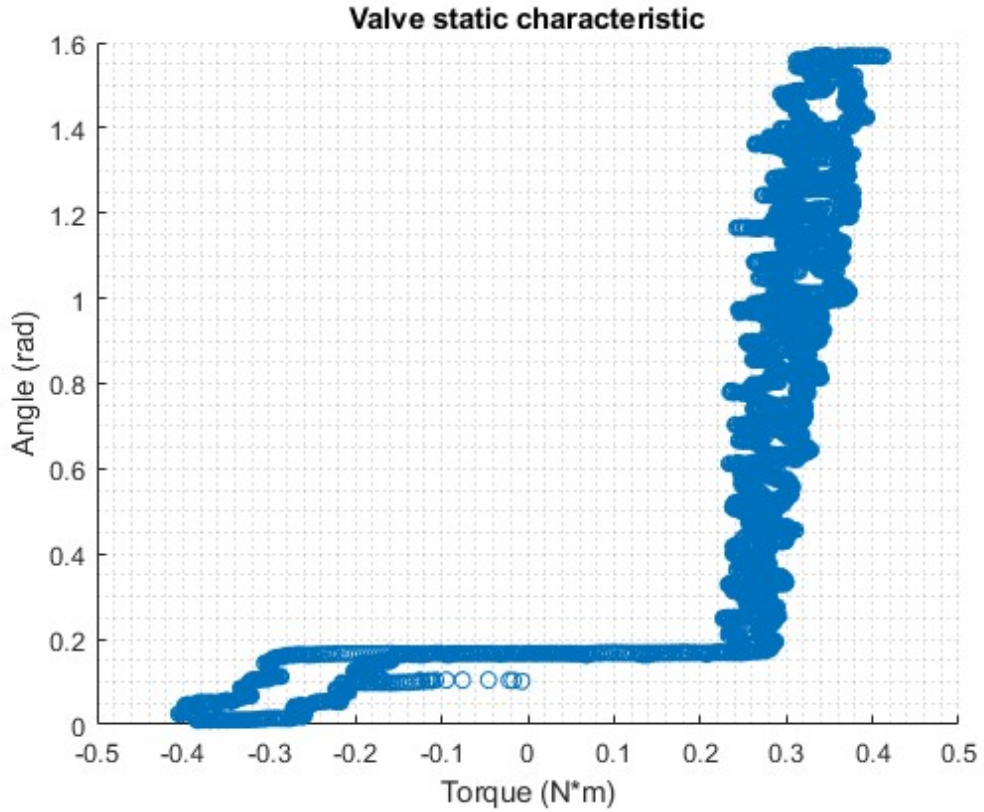


Figure 2.2: Valve static characteristic[4]

2.1.3 Dynamic characteristic

In order to derive the dynamic characteristic of the valve the useful torque at the plate is evaluated giving a sinusoidal set angle as input, then is from the contribution of the static parameters is subtracted to obtain only the dynamical torque.

$$T_{dyn} = B_L \dot{\theta} + I_{eq} \ddot{\theta} \quad (2.4)$$

Where B_L is the viscous coefficient of the plate only (without considering the motor), and I_{eq} is the equivalent inertia of the whole system with respect to the axis of rotation of the plate.

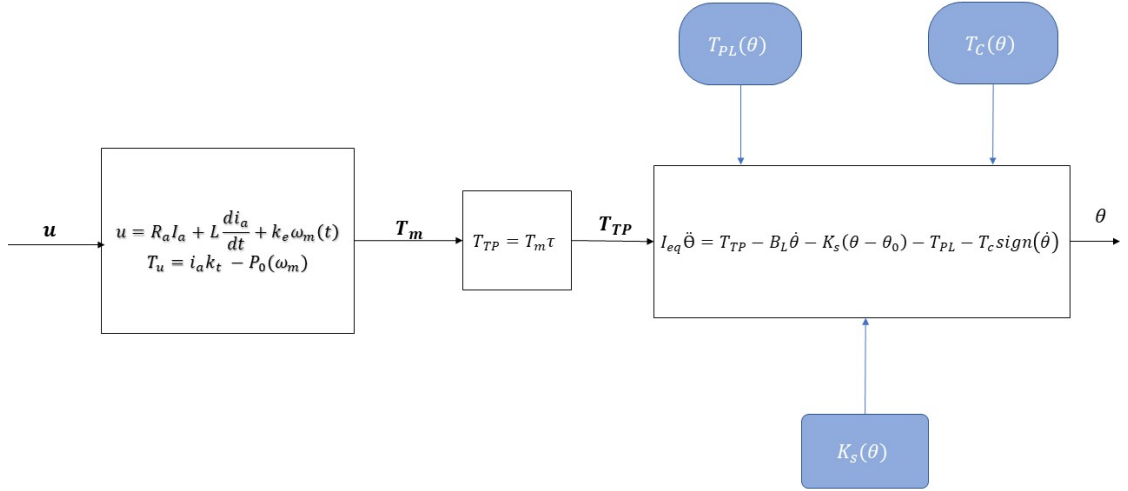


Figure 2.3: Block scheme of the ETV model used in the thesis

2.1.4 Parameter tables

In this paragraph are collected all the parameters values utilized to build the ETV model.

Table 2.1: Motor section parameters

Parameter	Value
R_a [ohm]	2.6342
L_a [H]	0.021795
k_e [V/(rad/s)]	0.01704

Table 2.2: ETV static parameters

Parameter	Angle	
	$\theta < \theta_0$	$\theta > \theta_0$
K_s [Nm/rad]	0.64785	0.074151
T_{PL} [Nm]	-0.32338	0.23889
T_c [Nm]	0.072206	0.01999

Table 2.3: Loss parameters and Dynamic parameters

Parameter	Value
T_{cm} [Nm]	2.2759e-03
B_m [Nm/(rad/s)]	1.1728e-06
C_{Dm} [Nm/(rad/s) ²]	3.1839e-11
θ_0 [rad]	0.1665
B_L [Nm/(rad/s)]	1.4242e-2
I_{eq} [Kgm ²]	6.9637e-4

2.2 Simulink model

The model used for design and simulation of the various controllers is built starting from the expressions used in the sections above to calculate the parameters, and translated into blocks.

The motor block is built in order to express the relation 2.1 expliciting the armature current. The inputs of this block are the control voltage (Armature voltage), and ω_m .

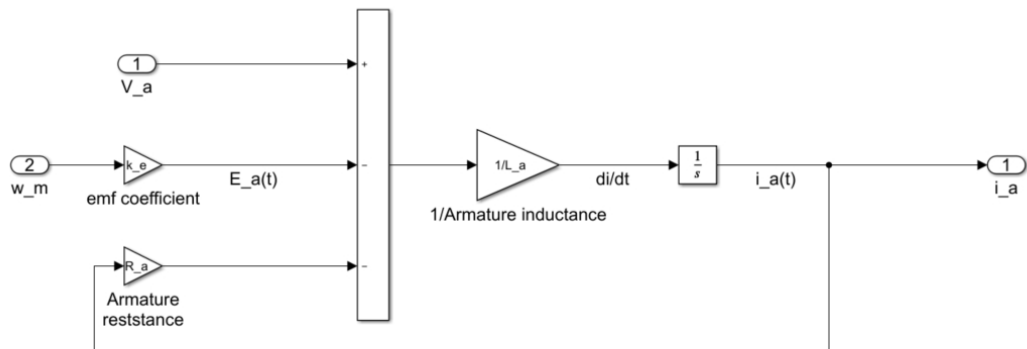


Figure 2.4: Simulink model of DC motor

Then to evaluate the useful torque at the motor the first two terms of 2.3 are used:

$$T_u = k_t i_a - P_0(\omega_m)$$

The block that evaluates T_u is then built considering also the expression to evaluate the dissipated power:

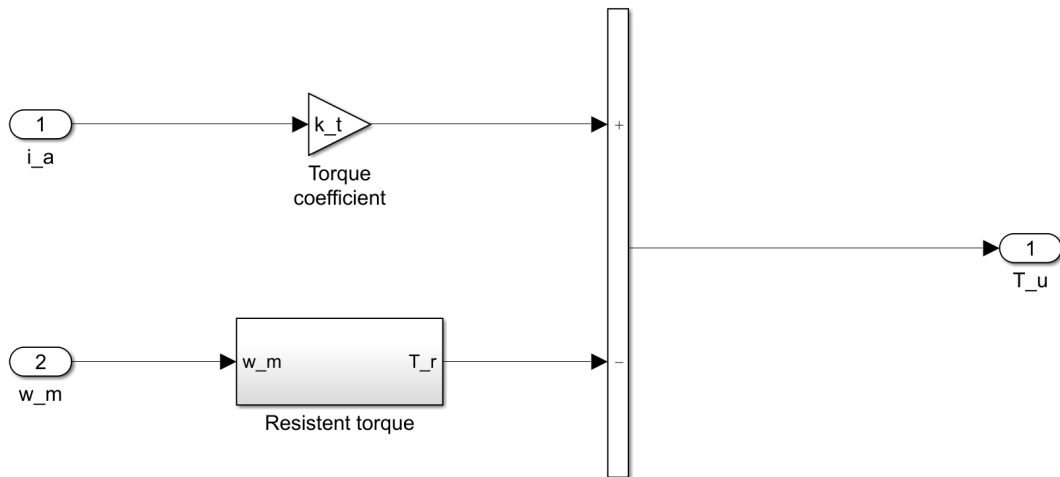


Figure 2.5: Rotor mechanical equilibrium block

Feeding the result to the reductor block, that perform the conversion of the useful torque at the motor to the useful torque at the throttle plate by simply multiplying it by the reductor ratio. This same block is used to obtain the ω_m from the

estimation of $\dot{\theta}$.

The last block exploits 2.3, and 2.4 in order to estimate the position of the valve, remembering that the dynamical torque has been obtained subtracting the contribution of the static parameters to the total torque at the plate, so the resulting total torque is:

$$T_{tp} = K_s(\theta - \theta_0) + T_{PL} + T_c \text{sign}(\dot{\theta}) + B_L \dot{\theta} + I_{eq} \ddot{\theta} \quad (2.5)$$

Isolating $\ddot{\theta}$ variable in 2.5 the following expression of the throttle plate acceleration is obtained:

$$\ddot{\theta} = \frac{1}{I_{eq}} [T_{TP} - B_L \dot{\theta} - K_s(\theta - \theta_0) - T_{PL} - T_c \text{sign}(\dot{\theta})] \quad (2.6)$$

After having defined the expression, the block that evaluates $\ddot{\theta}$ is built, and $\dot{\theta}$ and θ are obtained by integration. .

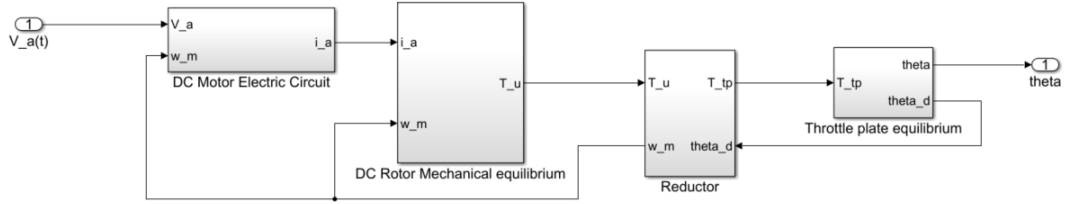


Figure 2.6: Full simulink scheme of the ETV model

2.2.1 Frequency response

A further analysis have been done on the linearized system identified by black box approach [4]. Then by means of Fast Fourier Transform(FFT) the bode diagram is built to represent the frequency response of the whole system. This kind of study is useful to understand the working frequency range of the ETV.

From the magnitude graph it is possible to notice the cutting frequency of the system. So for frequencies below 1 rad/s the magnitude remain constant. The performances degrade significantly above the cutting frequency, as well as the phase shift that reaches 90° slightly after that value.

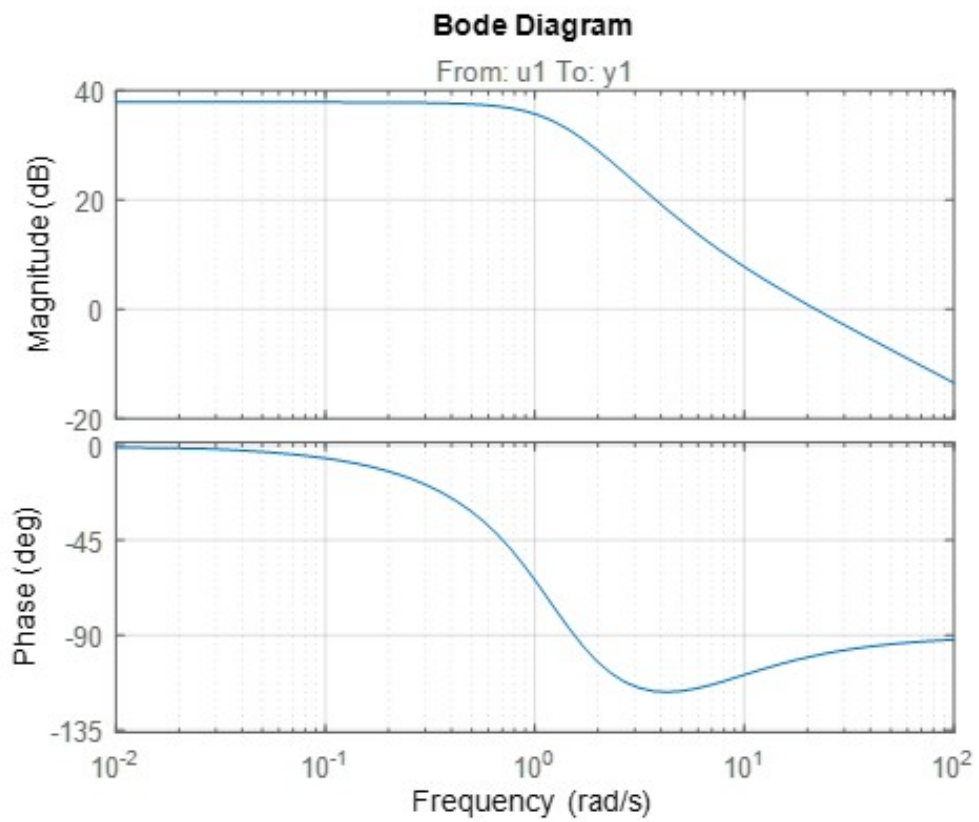


Figure 2.7: Full simulink scheme of the ETV model

Chapter 3

Control techniques

3.1 Youla-Coucera parametrization and FF compensation

In an early work done on the project [4], it was developed a controller based on the Youla-Coucera parametrization and a Feed-Forward compensation of the non-linearities.

The choice was done due to the simple implementation of the controller and the low computational effort needed.

3.1.1 Youla-Coucera parametrization

The objective of the Youla-Coucera parametrization is to find the family of controllers $K(s)$ that stabilize our closed loop system.

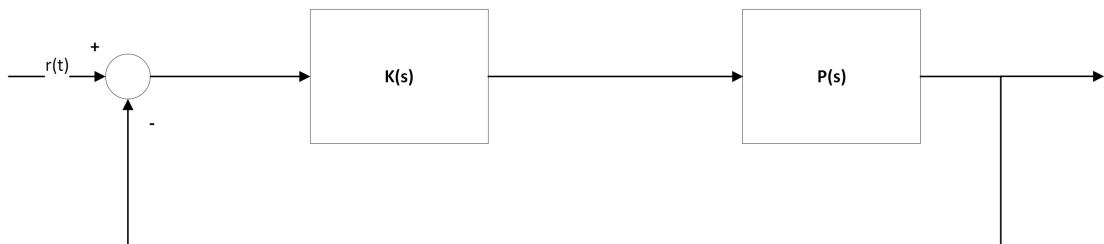


Figure 3.1: Closed loop scheme

The closed loop transfer function is given by:

$$T(s) = \frac{K(s)P(s)}{1 + K(s)P(s)} \quad (3.1)$$

Then, if $Q(s) = \frac{K(s)}{1+K(s)P(s)}$ is considered, the closed loop transfer function will be in the form $T(s) = Q(s) * P(s)$ and it is possible to find the expression of $K(s)$ in function of $Q(s)$:

$$K(s) = \frac{Q(s)}{1 - Q(s)P(s)} \quad (3.2)$$

$Q(s)$ is considered as the family of all stable filters, so if the plant is a stable one, the closed loop transfer function will be stable and a suitable controller $K(s)$, that stabilize the system, can be defined.

3.1.2 Plant inversion and shaping filter

Stability condition of $Q(s)$ is enough to ensure the stability of the entire control loop system. To obtain a stable $Q(s)$ the technique of plant inversion has been used.

As explained in [9] the plant inversion exploit the previous knowledge of the plant to obtain a suitable input for our system. Since the system is minimum phase (i.e. invertible), it is possible to produce the desired input by giving the desired output to the inverse of the plant, this is why the technique is called plant inversion. Then, in order to obtain the desired behavior of the closed loop system a so called shaping filter $F_q(s)$ is designed. The expression of $Q(s)$ is:

$$Q(s) = F_Q(s)P^{-1}(s) \quad (3.3)$$

The shaping filter $F_Q(s)$ is designed to be $F_Q(w) \approx 1$ for the working frequency range of the plant and to ensure that the $Q(s)$ filter is proper. This is achieved with the shaping filter having this form:

$$F_Q(s) = \frac{1}{(\tau s + 1)^{n_Q}} \quad (3.4)$$

Where the parameter n_Q is chosen to make $Q(s)$ at least biproper and τ is chosen in order to fulfill the specification of the project. Considering our design project the expression of $F_Q(s)$ has been defined as a low-pass filter:

$$F_Q(s) = \frac{1}{\frac{s}{w_c} + 1} \quad (3.5)$$

having $n_q = 1$ and $w_c = \frac{1}{\tau} = 5\text{rad/sec}$ for the specific case.

Moreover to avoid possible instability problem due to saturation of control input the controller has been inserted in an anti-windup loop.

3.1.3 Feedforward compensation

Since the system is highly non-linear due to the return spring and friction phenomenon (both dependent on the position of the throttle plate), a feedforward block has been added to compensate for this behavior. The total control action is then the sum of the control action produced by the controller previously computed and that of the feedforward block.

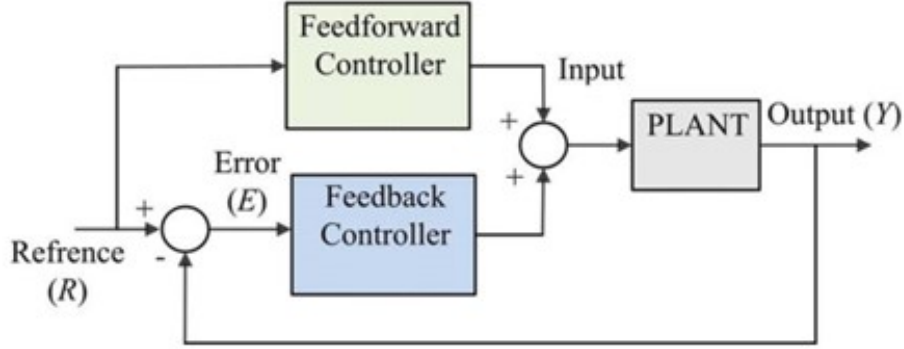


Figure 3.2: Feed Forward scheme

In order to evaluate the Feedforward control contribution we need to evaluate the torque contribution of the nonlinear actions. So is necessary to evaluate the compensation torque to be exerted by the DC motor and evaluate the voltage produced by that torque. The starting point is a direct correlation between the voltage and the nonlinear elements torque contribution. These informations can be derived from the ETV model starting from the expression of the armature voltage:

$$v_a(t) = R_a I_a + L_a \frac{di_a(t)}{dt} + k_e w_m(t) \quad (3.6)$$

That in the Laplace domain becomes:

$$V_a(s) = R_a I_a + sL_a I_a(s) + k_e \bar{w}_m(s) = (R_a + sL_a) I_a(s) + k_e \bar{w}_m(s) \quad (3.7)$$

Reminding that the torque constant is k_t it follows that:

$$I_a(s) = \frac{\bar{T}^{NL}(s)}{k_t} \quad (3.8)$$

The final expression of the armature voltage:

$$V_a(s) = \frac{R_a + sL_a}{k_t} T^{NL}(s) + k_e \bar{w}_m(s) = G_1(s) T^{NL}(s) + k_e \bar{w}_m(s) \quad (3.9)$$

The transfer function $G_1(s)$ is not proper (i.e. the order of the numerator is greater than the order of the denominator), so a Butterworth type lowpass filter of the second order $F_B(s)$ has been added so to obtain $G_1^* = G_1(s)F_B(s)$. The last element to consider in order to obtain the final transfer function is the gain of the driver that can be considered constant since the dynamics are much faster in comparison with the ETV.

The total command action is then provided by:

$$\bar{V}_{cmd}(s) = \frac{\bar{V}_a(s)}{K_{driver}} = \frac{G_1^*(s)}{K_{driver}} T^{NL}(s) + \frac{k_e}{K_{driver}} \bar{w}_m(s) \quad (3.10)$$

3.2 Sliding mode control

Sliding Mode Control (SMC) is a control technique derived from Variable Structure Systems (VSS) [10] in which a discontinuous action is applied to obtain different controllers depending on the state of the system.

The most advantageous feature of VSS is in fact the presence of a sliding motion. The goal is to bring our system towards the sliding surface despite the starting point in the state space and then maintain the system on the surface. The main idea is having different feedback controllers in opposite sides of a predefined surface of the state space in which I have the desired behavior for my system, bring the state points towards that surface and then maintain (slide) the system on it from then on [11]. The most important characteristics that make this type of controller suitable for a wide range of problems are:

- The insensitivity towards disturbances and parameter uncertainties (i.e. Robustness)
- The simple tuning of the parameters

Considering an example of a second order system taken from [11]:

$$\begin{cases} \dot{x}_1 = x_2 \\ \dot{x}_2 = b \cos(mx_1) + u \end{cases} \quad (3.11)$$

Selecting the following expression for the sliding surface,

$$s = x_2 + cx_1 = 0 \quad (3.12)$$

and the control law,

$$u = -cx_2 - \text{sgn}(s) \quad (3.13)$$

the behavior will be the one shown in figure 3.3 using these values for the parameters $c = 0.5$, $b = 0.75$, $m = 10$ and $x_{10} = 5$ and $x_{20} = 1$ as initial conditions.

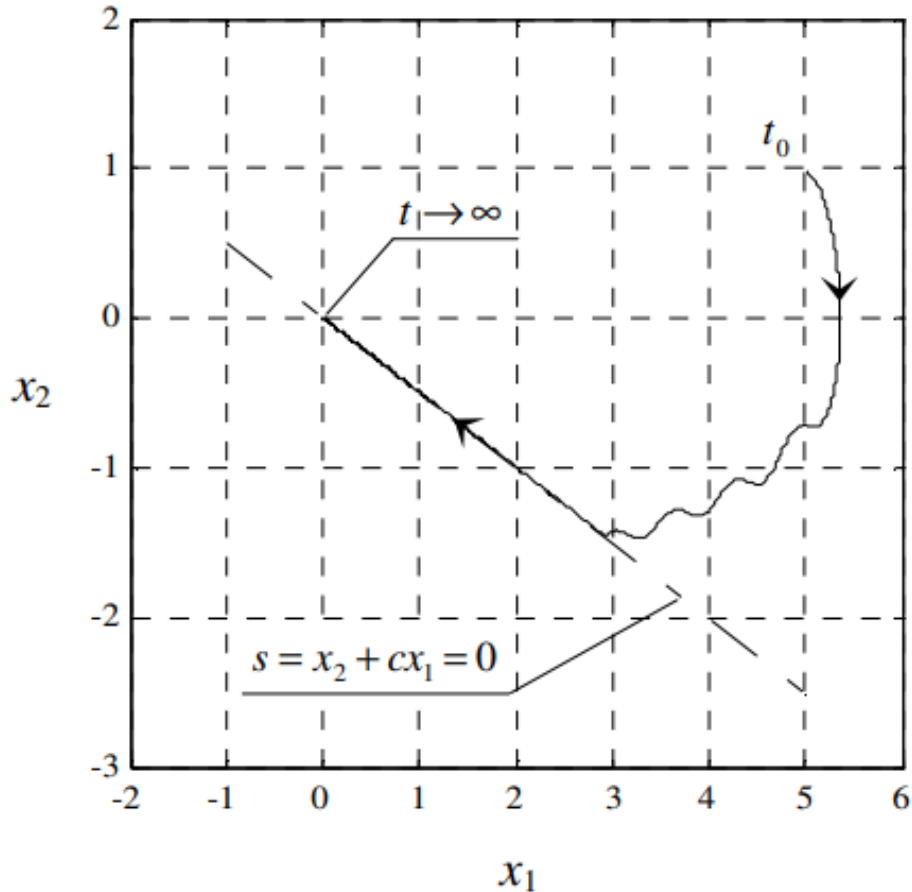


Figure 3.3: Phase trajectory of system 3.11 using control law 3.13

The so called reaching phase is clearly visible from t_0 until the trajectory touches the surface, then the sliding phase begins. In the example an ideal sliding mode occurs because an infinite switching frequency is considered. In real application finite switching frequency leads to oscillations near the surface causing a phenomenon called chattering.

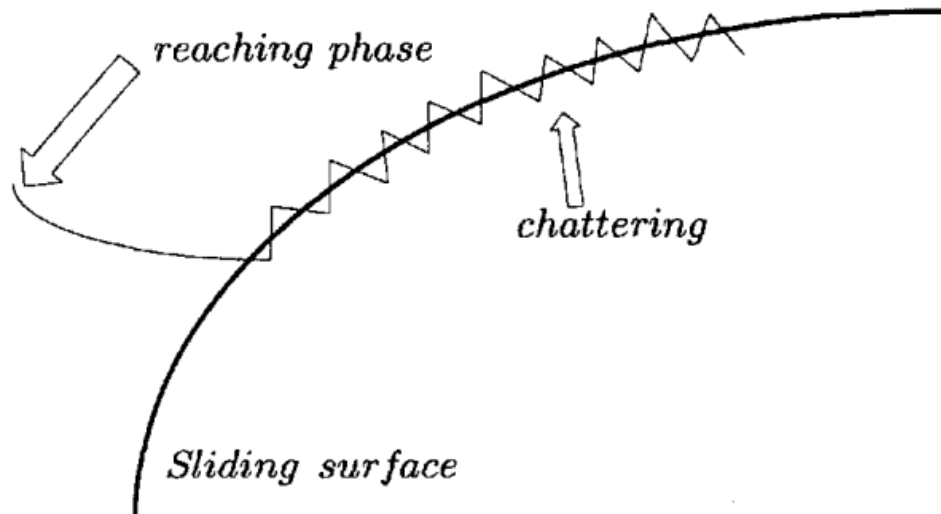


Figure 3.4: Chattering visualization

Chattering can lead to stability problems if is filtered, or lead to high effort for the actuator due to the high frequency oscillations.

3.2.1 General Framework

In order to derive the formulation of the controller for the ETV let's start from a general formulation of the problem.

Considering the following system:

$$\ddot{x} = f(x, t) + d(t) + u \quad (3.14)$$

where $f(x, t)$ is a nonlinear function of the states and time representing the modeled behavior of the system, $d(t)$ is a generic disturbance signal, and u is the control action.

The expression of the nonlinear function and the disturbance can be divided in the

contribution of two terms:

$$\begin{aligned} f(x, t) &= f_k(x, t) + \Delta f(x, t) \\ d(t) &= d_k(t) + \Delta d(t) \end{aligned} \quad (3.15)$$

$f_k(t, x)$ and $d_k(t)$ represent the known part of the function and the disturbance , while $\delta f(x, t)$ and $\delta d(t)$ represent the unknown uncertainty contribution. Consider then the state vector :

$$\vec{x} = \begin{bmatrix} x \\ \dot{x} \end{bmatrix} \quad (3.16)$$

and the error on the state:

$$\varepsilon = x - x_d \quad (3.17)$$

Were x_d is the desired state.

Our system can be then rewritten as:

$$\ddot{x} = f_k(x, t) + \Delta f(x, t) + d_k(t) + \Delta d(t) + u \quad (3.18)$$

3.2.2 Choice of the sliding surface

There is no general rule to find the sliding surface. The choice is done considering which surface will be useful to reach the desired behavior.

Since our goal is to reach a desired angle set the proper choice would be:

$$S = \dot{\varepsilon} + \lambda\varepsilon \quad (3.19)$$

When the system is sliding on the surface, equation 3.19 is equal to 0, this implies:

$$\dot{\varepsilon} + \lambda\varepsilon = 0 \implies \dot{\varepsilon} = -\lambda\varepsilon$$

Solving the simple differential equation it is obtained:

$$\varepsilon(t) = e^{-\lambda(t-t_0)}\varepsilon(t_0)$$

Consequently $\varepsilon(t)$ will tend to 0 as $t \rightarrow \infty$ for any $\lambda > 0$

3.2.3 Control action formulation

The relative degree of the system is two, since it is necessary to derive the output, (that in our case is the throttle plate angle and corresponds to the first state) , 2 times before the control action u appears in the expression.

So, considering the sliding surface previously defined and taking the derivative the following expression is obtained:

$$\dot{S} = \dot{\varepsilon} + \lambda\dot{\varepsilon} = \ddot{x} - \ddot{x}_d + \lambda\dot{\varepsilon} \quad (3.20)$$

substituting the expression 3.18 in the 3.20 the following expression is obtained:

$$\dot{S} = f_k(x, t) + \Delta f(x, t) + d_k(t) + \Delta d(t) + u - \ddot{x}_d + \lambda\dot{\varepsilon} \quad (3.21)$$

So the control action is selected in such a way to cancel out the known terms:

$$u = -f_m(x, t) - d_m(t) + \ddot{x}_d - \lambda\dot{\varepsilon} + \nu \quad (3.22)$$

The term ν is designed in order to deal with uncertainties and to fulfill the reachability condition (chapter 1 of [12]). To ensure $S \rightarrow 0$ in finite time we need to know at least the upper bound of the uncertain terms :

$$\begin{aligned} |\Delta f| &\leq \alpha(x, t) > 0 \\ |\Delta d| &\leq \beta(t) > 0 \end{aligned} \quad (3.23)$$

Using the Lyapunov method to verify the reachability condition, and so having $S\dot{S} < 0$ it follows:

$$\nu = -(\eta + \alpha + \beta)sign(S) \quad (3.24)$$

It follows that $S\dot{S} \leq -\eta S sign(S) < 0$ for every $\eta > 0$, ending up with the final expression for the control u :

$$u = -f_m(x, t) - d_m(t) + \ddot{x}_d - \lambda\dot{\varepsilon} - (\eta + \alpha + \beta)sign(S) \quad (3.25)$$

3.2.4 Chattering compensation

Many ways has been studied in order to reduce or eliminate chattering.

A possible solution presented in [11] is to substitute the *sign* function with a continuous one such as saturation function. This reduces chattering as the discontinuous term is not present anymore but the switching variable will converge to an interval that depends on the function parameter.

Another function that is possible to use for the purpose is the hyperbolic tangent, that is smooth and continuous. So the discontinuous term is substituted by :

$$\nu = -tanh(\eta S) \quad (3.26)$$

High value of the η parameter makes the *tanh* more similar to the *sign* function, increasing the slope in the neighborhood of the origin, so i can tune this parameter making the control action smoother provided that the performances parameters are still satisfied.

3.3 Super Twisting sliding mode algorithm

To overcome the problem of chattering other methods have been studied in literature, one of the most important is the Higher Order Sliding Mode theory. The HOSM aim at optimize the discontinuous action contribution to chattering by working on higher order derivative of the sliding surface in such a way that[12]:

$$S = \dot{S} = \ddot{S} = \dots = S^{(r-1)} = 0 \quad (3.27)$$

Where r is the sliding order of the system, and indicates the order of the sliding surface in which is present the discontinuous action.

In order to be effective the sliding order considered must be higher than the relative degree of the system, so for a system of the second order, a sliding order equal to 3 has to be considered.

The higher is the sliding order with respect to the relative degree, the smoother will be the response. This is due to the fact that the discontinuous action, present in the r^{th} order sliding surface, is then integrated r times to obtain the actual control signal, and so the u signal will be continuous.[13]

Various algorithm has been developed to exploit HOSM. One is the Twisting algorithm, that is the first known algorithm to be exploited, that take the name from the phase portrait of the algorithm considered as a system[12] that converges to the origin 'twisting' around it infinite times. Instead in [14] a version with an adaptive algorithm is presented, stressing out the fact that the only design parameter to be known are the bounds on the uncertainties.

Another algorithm is the Super Twisting Sliding Mode Control one. This algorithm as the TA previously mentioned has only to satisfy some constraint considering the uncertainty bounds, and only need informations about sliding surface S .

3.3.1 Super Twisting Algorithm

The STSMC algorithm comprise two terms, the first is the actual control action, the second one is the derivative term that contains the discontinuous action. The mathematical formulation is the following[7]:

$$\begin{cases} u = -K|S|^{\frac{1}{2}}\text{sign}(S) + \nu \\ \dot{\nu} = -\alpha\text{sign}(S) \end{cases} \quad (3.28)$$

Were λ and α are the parameters to be tuned, and the sliding surface S is defined as 3.19

In order to ensure convergence in finite time of the sliding surface S , some constraints on the second derivative \ddot{S} , must be satisfied. Considering the expression of \ddot{S} as:

$$\ddot{S} = h(x, t) + g(x, t)\dot{u} \quad (3.29)$$

The functions $h(x, t)$ and $g(x, t)$ are unknown but are bounded by some constant quantity in this way :

$$\|h(x, t)\| < A_m, \quad \Gamma_m \leq \|g(x, t)\| \leq \Gamma_M$$

The sufficient conditions can therefore be expressed as:

$$\begin{aligned} K &> \frac{A_m}{\Gamma_m} \\ \alpha &> \frac{4A_m}{\Gamma_m^2} \cdot \frac{\Gamma_M(K + A_m)}{\Gamma_m(K - A_m)} \end{aligned} \tag{3.30}$$

Chapter 4

Numerical implementation

The implementation of the classical Sliding Mode controller and the Super Twisting Sliding Mode controller has been done in Simulink[®]. Then the controllers are tested using the model of the valve (model in the loop) using different wave signals to catch the different behaviors. The result are then used to compare the controller performance with respect to the controller previously developed in the project for TTech.

4.1 Sliding Mode implementation

The main element for the design of the SMC is the definition of the sliding surface that in our case is defined in 3.2.2. In order to be able to evaluate the error mathematically a representation of the model in the following form is needed:

$$\ddot{x} = f(x) + g(x)u \quad (4.1)$$

In which x is our state variable having $x_1 = \theta$ and $x_2 = \dot{\theta} = \omega_t$.

Considering this state space representation the model will be expressed in this way:

$$\dot{\mathbf{x}}_2 = \frac{1}{I_{eq}} \left[\frac{k_t \tau}{R} \mathbf{u} - \frac{k_e k_t \tau^2}{R} \mathbf{x}_2 - (T_{cm} + B_m \tau \mathbf{x}_2 + C_{dm} \tau^2 \mathbf{x}_2^2) \tau^2 \mathbf{x}_2 - K_s (\mathbf{x}_1 - x_0) - T_{PL} - T_c \text{sign}(\mathbf{x}_2) - B_L \mathbf{x}_2 \right] \quad (4.2)$$

From this representation of the model we can derive the f and g of the equation

4.1 and evaluate the needed control action. The expressions are:

$$f = \frac{1}{I_{eq}} \left[-\frac{k_e k_t \tau^2}{R} \mathbf{x}_2 - (T_{cm} + B_m \tau \mathbf{x}_2 + C_{dm} \tau^2 \mathbf{x}_2^2) \tau^2 \mathbf{x}_2 - K_s (\mathbf{x}_1 - x_0) - T_{PL} - T_c \text{sign}(\mathbf{x}_2) - B_L \mathbf{x}_2 \right] \quad (4.3)$$

$$g = \frac{1}{I_{eq}} \frac{k_t \tau}{R} \quad (4.4)$$

The next step is the definition of the sliding surface as exploited in 3.2.2. So considering our system variables and substituting them in equation 3.19 it is obtained the following expression :

$$S = x_2 - \dot{x}_d + k_2(x_1 - x_d) \quad (4.5)$$

Thus obtaining a control action of the form

$$u = -\frac{1}{g}(-f + \ddot{x}_d - \lambda \dot{\epsilon}) - \eta \text{sign}(S)$$

In order to avoid integration problems using the matlab function block in Simulink[®], the discontinuous parameters of the ETV model have been evaluated using a hiperbolic tangent function to make them continuous. The solution adopted is the following :

$$K_s = \frac{(K_s^+ - K_s^-)}{2} \tanh(C(\theta - \theta_0)) + \frac{(K_s^+ + K_s^-)}{2} \quad (4.6)$$

$$T_{PL} = \frac{(T_{PL}^+ - T_{PL}^-)}{2} \tanh(C(\theta - \theta_0)) + \frac{(T_{PL}^+ + T_{PL}^-)}{2} \quad (4.7)$$

$$T_C = \frac{(T_C^+ - T_C^-)}{2} \tanh(C(\theta - \theta_0)) + \frac{(T_C^+ + T_C^-)}{2} \quad (4.8)$$

Where K_s, T_{PL}, T_C are the nonlinear parameters, and the apex + or - represents respectively the parameter value for values of θ greater than θ_0 and for values smaller than θ_0 . The coefficient C regulates the slope of the hyperbolic tangent function.

The controller algorithm has been implemented exploiting the matlab function block in Simulink[®]. In t

The parameters are chosen by trial and error considering the trade-off between rising time, steady state error , chattering and control action effort. So in such a way to have good tracking performances without having a too high control action.

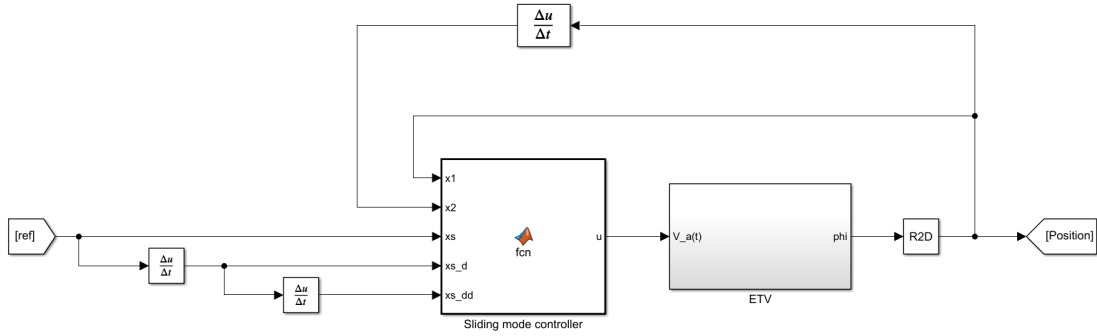


Figure 4.1: Simulink implementation of SMC

4.1.1 Integration problems

The evaluation of the control action gave problem in the integration of the model for simulations. The value diverges in presence of a variation of the signal(step, ramp ,sine), ultimately this render the system non-usable at the current state. Neither filters or saturation block fixed the problem.

4.2 STSMC implementation

The block scheme implementation is similar to that of the classical SMC , in the matlab function block is written the algorithm of the STSMC algorithm that is expressed in 3.28.

The code used for the controller,containing the parameters definition and the implemented algorithm is shown in appendix A.

The parameters values have been chosen by trial and error procedure in order to have a good trade-off between rising time performances, steady state error and control action.

4.2.1 Simulink scheme functional description

In this section is presented a detailed overview of the simulink scheme of the Super Twisting Sliding Mode Controller.

The scheme is composed by four different types of blocks. There are three derivative blocks , one integrator , the actual controller and the ETV model. Then there is the arrow representing the input reference signal. In detail:

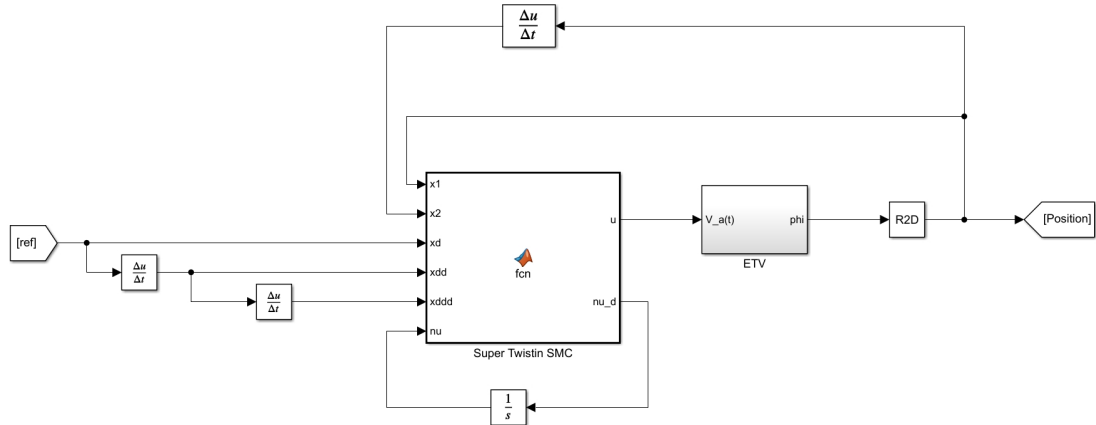


Figure 4.2: Simulink implementation of STSMC

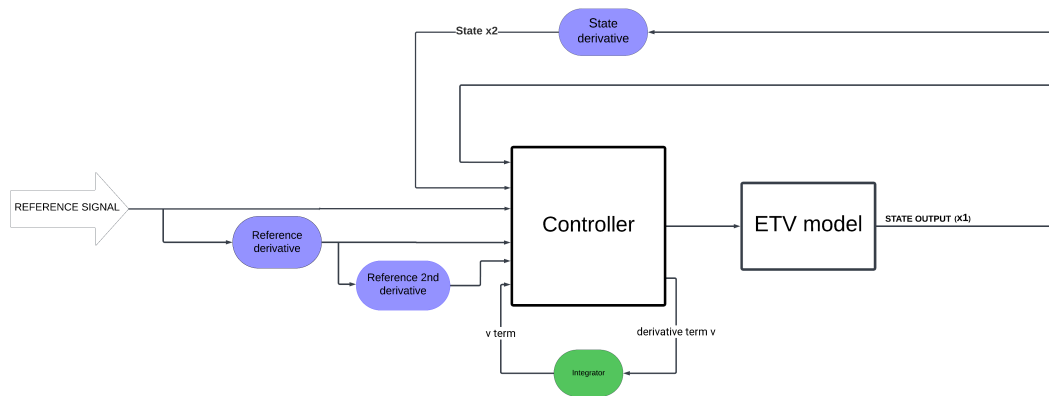


Figure 4.3: Descriptive scheme for 4.2

- **ETV model:** this block represents the model of the system used for simulation and tests
- **Controller:** this block takes as input the states of the system, the reference signal and its first two derivatives and the ν term. It uses all these input to evaluate the supertwisting algorithm as shown in the matlab code : all the constant parameters are declared first , then the position error is evaluated and the sliding surface is defined and lastly the control law is described. The outputs of the block are the actual control law u and the term $\dot{\nu}$
- **Integrator:** This block is used to evaluate the ν term starting from $\dot{\nu}$, that is

the term containing the discontinuous action.

- **State derivative:** this block is used to evaluate the second state of the system (rotational speed) from the output of the system that is the only first state (angle position)
- **Reference derivative(1st and 2nd):** these two derivative blocks are used to evaluate the first and second derivative of the reference signal needed for the evaluation of the algorithm. They are used to evaluate first and second derivative of the position error.

4.2.2 Step simulations

In order to evaluate the time response of the system a set of step signal have been used as reference. To fully evaluate the behavior, the step functions are chosen with values between 0 and 90 degrees with steps of ten to span the majority of the valve working points. The criterion chosen to evaluate the settling time is considering the time needed for the output to reach and stay within an error band of $\Delta\theta = 3^\circ$.

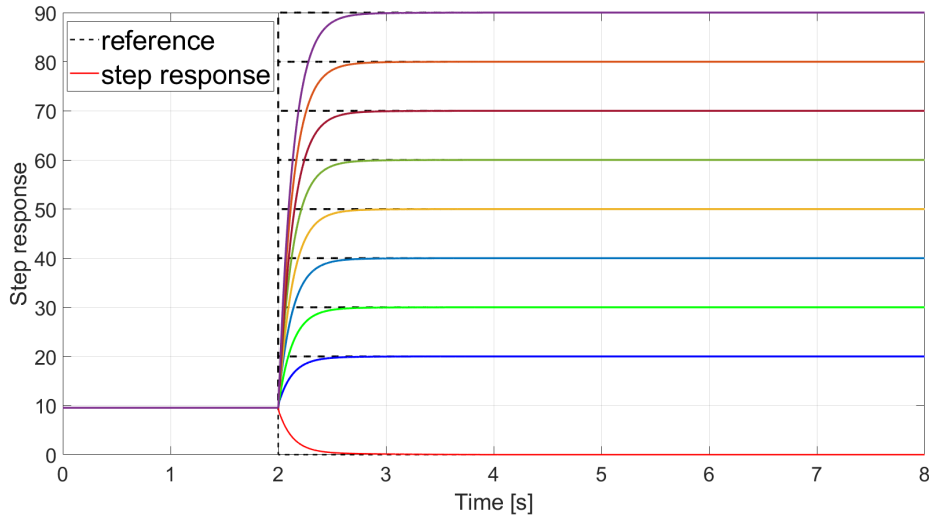


Figure 4.4: Step response of STSMC

Settling time

As it is possible to see in image 4.4 representing all the various step responses, the STSMC does not cause overshoot in the output response, therefore the settling time is equivalent to the rise time if we consider the same $\Delta\theta$ for the evaluation of these criteria. In table 4.1 the settling time $t_s^{\Delta\theta}$ are grouped for all step simulations.

Table 4.1: Settling times of STSMC

Set angle [°]	Settling time [s]
0	0.157
20	0.157
30	0.252
40	0.302
50	0.347
60	0.375
70	0.404
80	0.422
90	0.442

Steady state error

After the analysis on the settling time, the steady state error (e_{ss}) is taken in exam. From the step simulation graph (4.4) it is observable that the steady state error appears to be small for all the angles range. Checking the data results it is visible that $e_{ss} \approx 10^{-4}$ for all step simulation, that is very low for our application. By zooming closely some high frequency oscillations are present in that trait, but the working frequency of the ETV is much lower so this will not effect the results.

Small step simulations

Near the limp home position (or rest position) of the ETV the return spring cause a strong non linearity. So to verify the robustness of the controller in this strong nonlinear region some simulation have been performed considering a different set of step signals. The angles used for the simulation sweep from 5° to 15° in order to span all the neighborhood of the rest position of the valve. The response is stable for all steps and the steady state error is comparable with the value found for the bigger step simulations. In figure 4.6 are represented all the simulations, having the dotted line as the reference step signal.

4.2.3 Stair signal simulation

For this test an up-down stair signal is used to simulate a situation more similar to the real working behavior. The whole response, present in figure 4.7 shows a

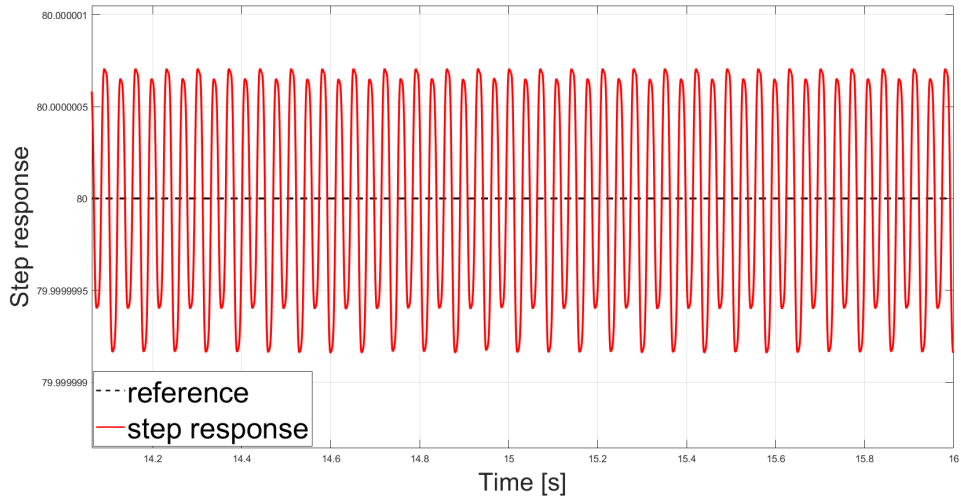


Figure 4.5: Zoom of the signal and set angle of 80° at steady state

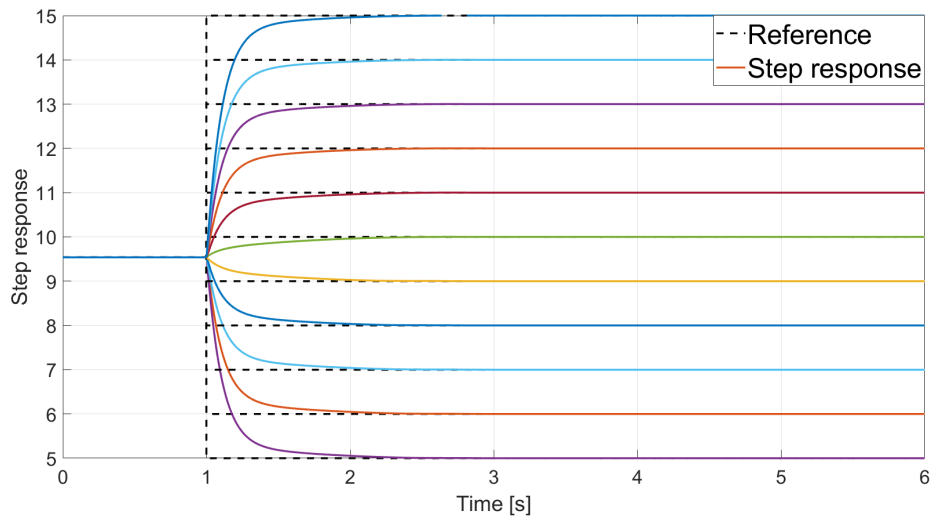


Figure 4.6: Step response for various small angle set

good behavior in terms of tracking performances. The error behavior is shown in figure 4.8 and despite the presence of the $\pm 10^\circ$ spikes, that are inevitable due to the intrinsic nature of the simulation, it has a good trend.

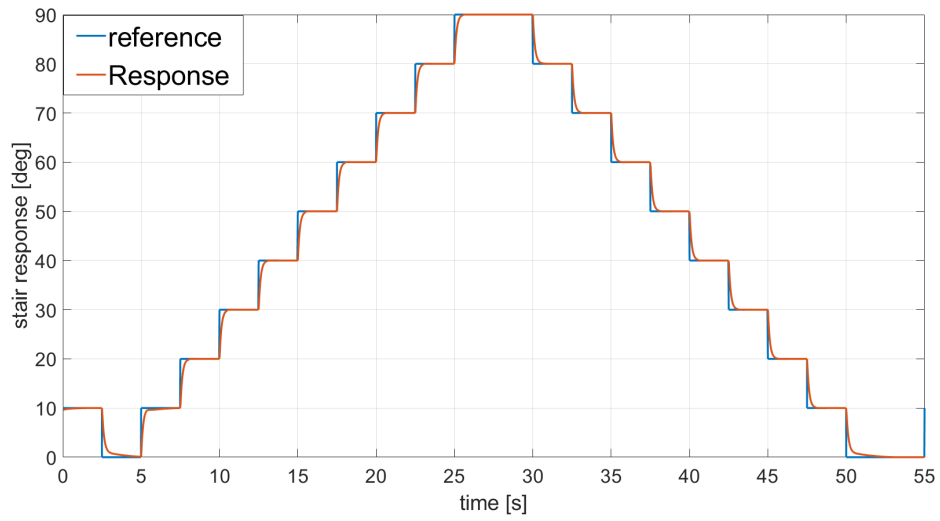


Figure 4.7: Stair signal simulation

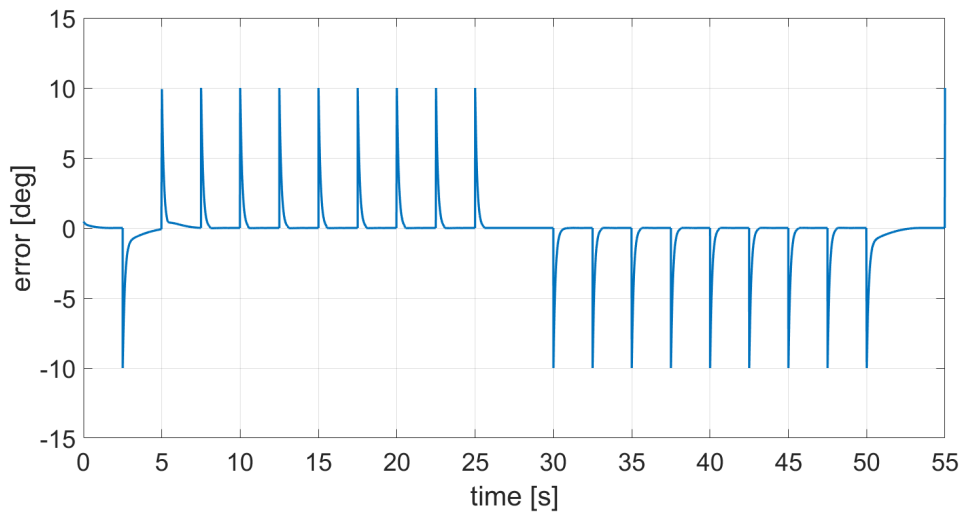


Figure 4.8: Stair signal simulation error

4.2.4 Sine wave simulations

The test done with a sinusoidal signal serve the purpose of verifying the behavior for different velocity of variation of the set angle. The test have been done with different angle and frequencies. The signal used is of the form:

$$\theta_{set} = \theta_{offset} + \theta_a \sin(\omega t)$$

Changing the frequency of the set it is visible how the tracking performance degrade around the frequency of 300 rad and above. But since the valve has a much lower frequency working band the performances are not affected by such behavior.

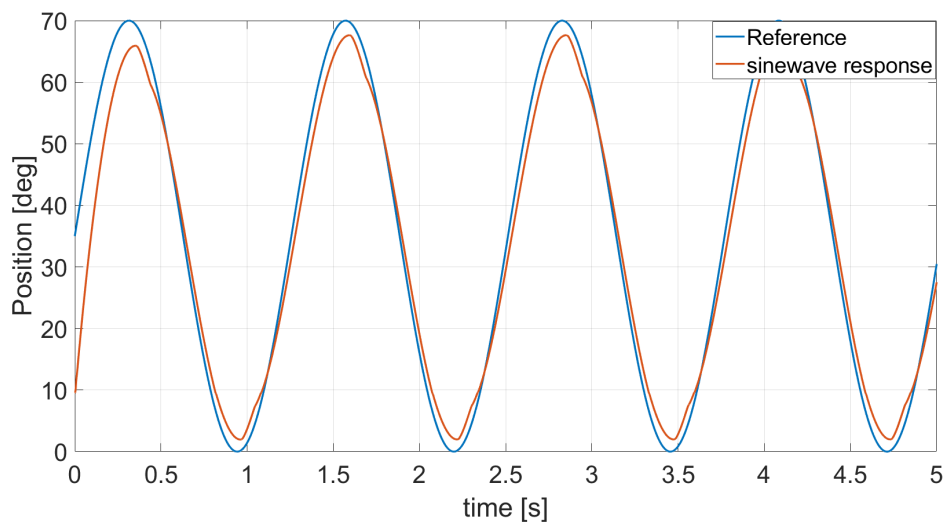


Figure 4.9: Simulation with a sinewave at 5rad frequency

4.2.5 Triangular wave simulation

The triangular wave is used to simulate the case of an ascending and descending linear ramp. This kind of signal serves the purpose of testing the valve in a condition of constant velocity.

As we can see from image 4.10 the tracking is stable and precise during the entire trait. Also the error is very small as the reference (dotted line) and the output of the system (red line) almost overlaps.

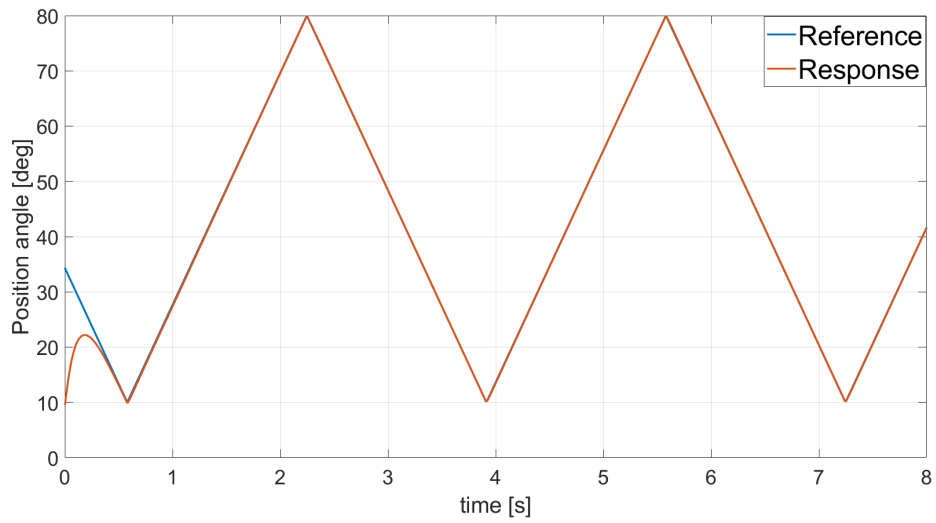


Figure 4.10: Triangular wave simulation

Chapter 5

Simulation tests and comparisons

The primary goal of this chapter is to provide a detailed comparison between the controllers that were examined. The aim is to highlight the differences in terms of performance and behavior. The analysis is conducted in order to provide an understanding about the possible improvement brought by the new formulated system.

5.1 Testbench characteristics

In the previous study, the measurement of the Youla-Coucera controller was conducted through experimental testing using a dedicated experimental testbench as shown in image 5.1. The scheme depicts the interconnections among the various elements and visually illustrates the linkages between the components, providing a clear overview of their connections.

The elements and devices that correspond to the various blocks of the scheme are the following:

- Control and signal acquisition device (National Instrument myRIO 1900)
- Driver for providing the control to the valve DC motor (Electromen EM-176A)
- Current sensor (Texas Instruments INA 250A4)
- Two RC low-pass filters with nominal cutting frequency of 1421Hz
- 12 VDC generator

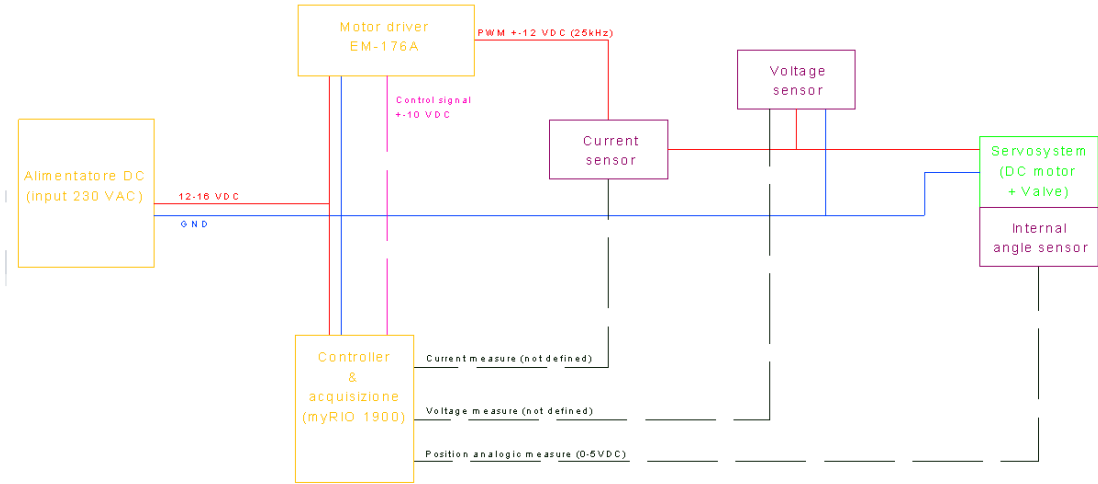


Figure 5.1: Testbench scheme

The ETV under examination is already provided with an internal position sensor. The myRIO device is used to acquire all the characteristic state variable of the system. The information acquired consider not only the position of the throttle plate , that is fundamental for the correct functioning of our feedback system, but also saves the information about current and tension at the poles of the DC motor. The data collected have been used to evaluate the model of the Electronic Throttle valve as extensively reported in chapter 2.1. The driver EM-176A generate the command signals for the motor. It provides two different inputs :

- An analogic signal proportional to the output voltage of the driver
- A logic signal providing the direction of rotation of the motor

The acquisition is done iterposing a voltage divider between the motor and the myRIO device. This is because the nominal power supply voltage for the motor is 12V in DC , instead the data collection device is able to measure voltage in the range of $\pm 10V$. A lowpass filter is needed to measure the PWM signal of the driver. The cutting frequency of 1421Hz is designed to not interfere with the test done on the valve that has natural frequency of 1Hz. Instead the current sensor has a gain of 2V and it is supplied with a 15V voltage. Since the output volatage range is between 0 – 15VDC in order to measure negative currents it is possible to add a reference voltage (in this case 5V)to change the possible current measurement range to $[-2.5,5]A$. The position measurement was carried out using the valve’s internal sensor, which operates at a 5VDC voltage and provides a 0 – 5VDC output range for the selected configuration. The sensor’s output is ratiometric, with a characteristic equivalent to 0.952% of the supply voltage per degree of disk

rotation. Regarding the control action exerted by the myRIO, it is important to consider that its analog output operates within a $\pm 10VDC$ range. However, the motor driver's output is in the $\pm 29VDC$ range, exceeding the motor's nominal voltage of $12VDC$. To accommodate this, the command signal has been limited. Furthermore, the motor speed reference has been split into its absolute value and sign. The first signal corresponds to a positive analog output from the myRIO, while the rotation direction is determined by a second signal output from the myRIO and input to the driver.

5.2 labVIEW implementation of Youla-Coucera configuration

Before collecting the experimental data the system has to be designed in the labVIEW environment. In image B.1 is implemented the calculation of the nonlinear discontinuous term that are needed to evaluate the feedforward action.

In figure 5.2 is shown the implementation of the feedforward action that is then combined with the closed loop controller(5.3) to generate the total control action. In the operative cycles of execution, all the important variable are measured

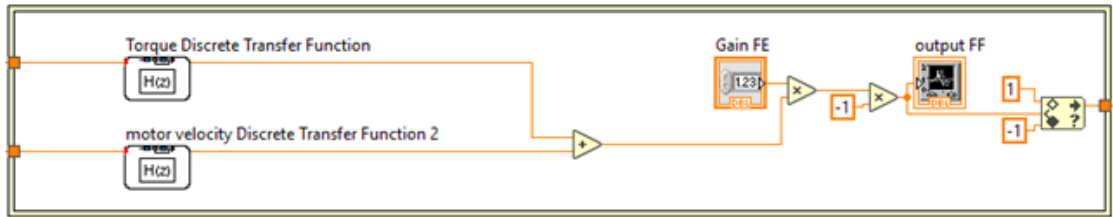


Figure 5.2: labVIEW representation of Feed Forward control action

considering a time reference and the signal value:

- Set position
- Output angle (measured by the valve Hall sensor) to evaluate the position error needed by the feedback
- The derivative of the signals are evaluated with a filter of this form : $\frac{s}{s+w_d+1}$

5.3 Step response comparison

The step response simulation is the most important test to evaluate the performances of a system. Understanding the system's response to an abrupt input change is

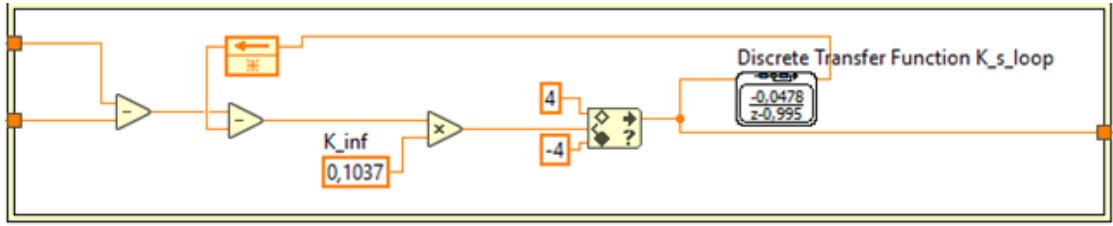


Figure 5.3: labVIEW representation of closed loop control action

crucial in assessing the stability of the overall control loop , as well as the ability to arrive at a steady state value. In order to compare the Youla-Coucera controller with the Super Twisting Sliding Mode one the responses to various steps have been taken in account. The main performance criteria considered are the settling time and the steady state error. To give an indicative and initial comparison, the experimental results of the Youla-Coucera controller are compared with the simulations done in Simulink[®] of the STSMC .

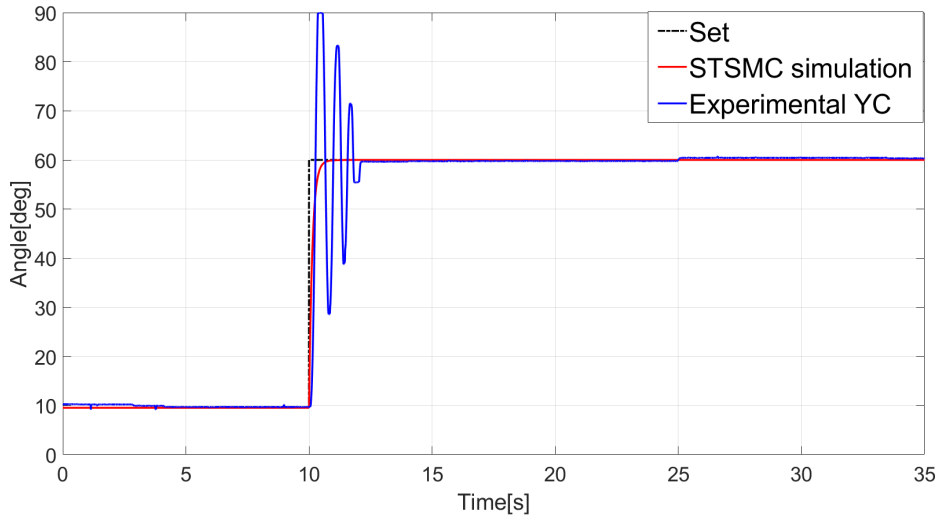


Figure 5.4: Step response comparison for 60 degree angle

The first thing that is possible to notice in image 5.4 is the big overshoot present in the experimental step response of the Youla-Coucera controller. Instead the STSMC arrives at steady state without any oscillation. This problem increase with the amplitude of the step for the Youla-Coucera configuration, but for the 80 and 90 degree step angle is limited by the physical limitation of the valve when it is fully open at a square angle. Having a response without overshoot may avoid the situation where the throttle plate hits the stop position, either in fully open

or fully closed scenario. Avoiding oscillations in the response increase the overall performances of the system, both regarding fuel consumption and driving comfort. The rising time, as we can see from image 5.5, is smaller for the STSMC far almost all angle set, excluding 80 and 90 degree angle, for which the settling time is decreased for the same reason that limits the overshoot for the higher angles.

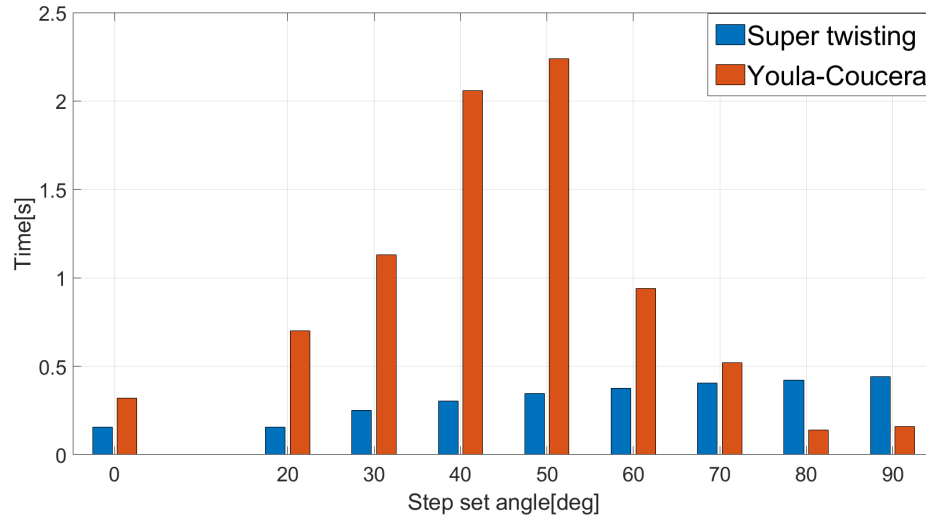


Figure 5.5: Settling time comparison

Regarding the steady state error, as seen in section 4.2.2 ,for the Super Twisting Sliding Mode Controller is negligible compared with the Youla-Coucera.

5.4 Stair response comparison

The comparison of the result of this test is done to highlight the different behavior when the input signal has abrupt changes of angles that are not too high.

In image 5.8 it is clearly visible the presence of overshoot in the Youla-Coucera simulation, as in the step response simulation. The STSMC response is smoother and the error, seen in image 4.8, is reasonable compared with the error error characterizing the YC(image 5.9).

5.5 Sine response comparison

In this last simulation the aim is to analyze the different behavior obtained in response to a sinusoidal signal. The main issue, visible in image 5.11 is the flat

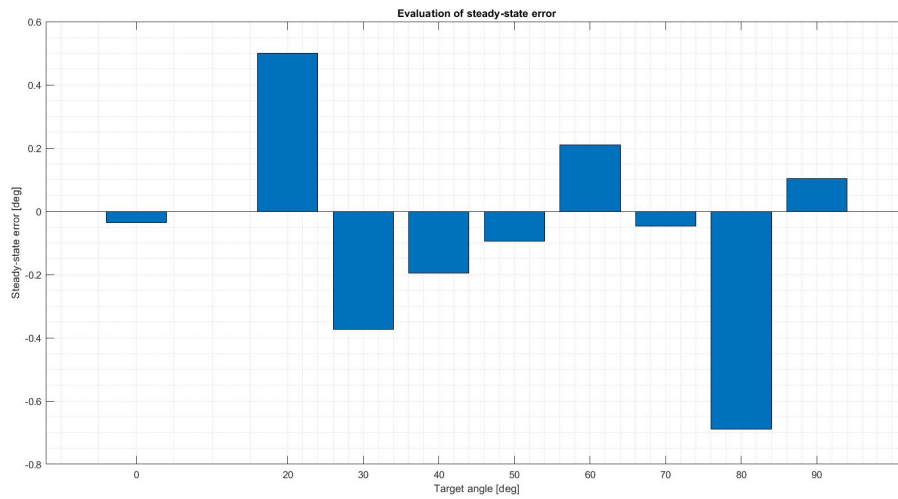


Figure 5.6: Steady state error using Youla-Coucera controller

trend near the fully closed position. This behavior, not present in the STSMC, is due to the inability of the YC controller to follow small angle reference.

In fact it is clear from a test with a sinusoidal wave oscillating between a set position of 20 to 70 at a frequency of 1Hz that even though the tracking has a bit of delay it is reasonably smooth.

5.6 Final considerations

Simulation and comparisons are an important step to do to understand the different characteristics and find the better solution for our purposes. In this chapter the main goal was to present an indicative comparison between the previous study conducted on the topic and the new model presented in this work. Even though the similarity and contrasts are seen between the experimental data collected in the antecedent report and the Simulink[®] assessments done on the new model, the main intent was to give an overview on the possible improvements brought by STSMC.

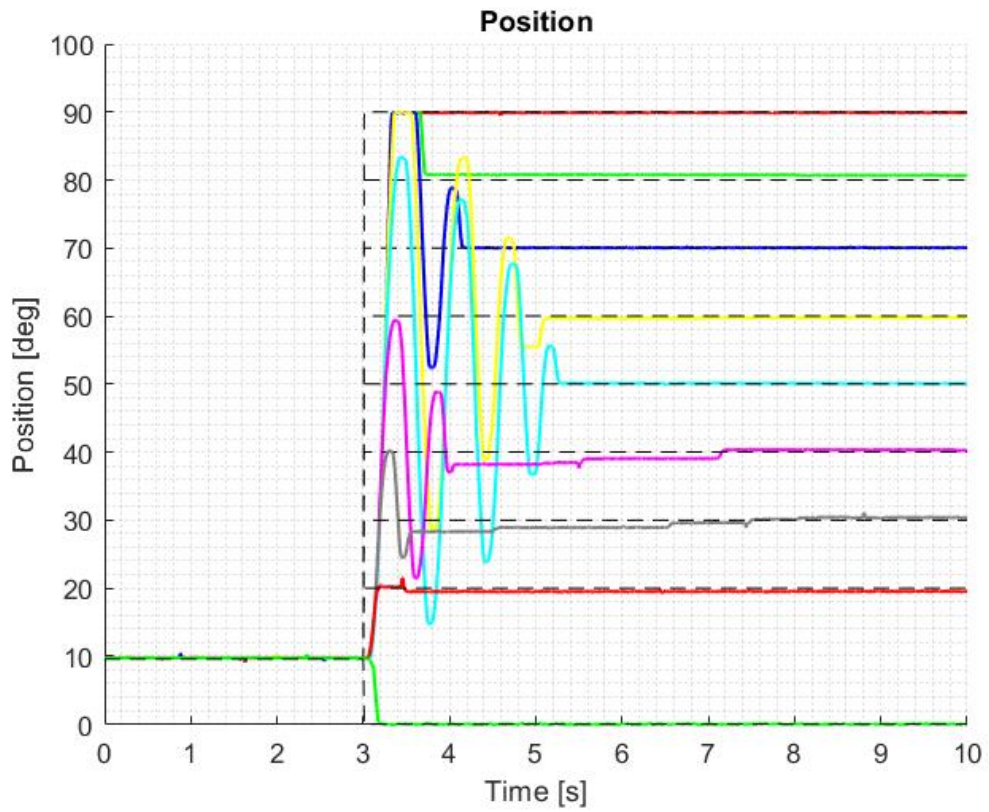


Figure 5.7: Step simulation for Youla-Coucera system

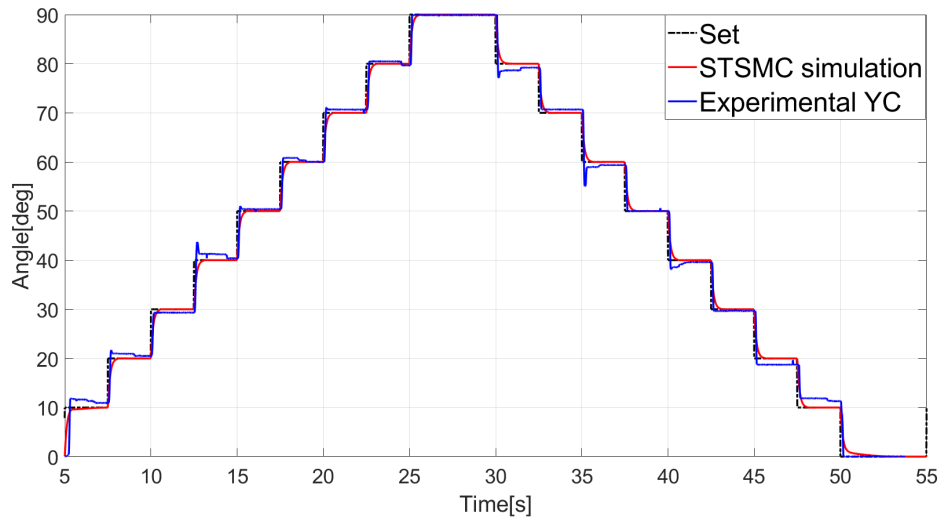


Figure 5.8: Stair simulation comparison

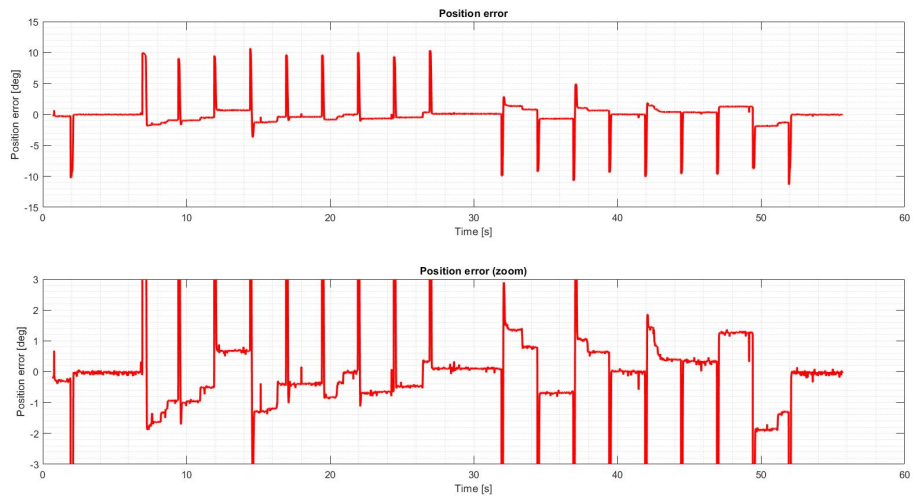


Figure 5.9: Stair simulation error of Youla-Couceru

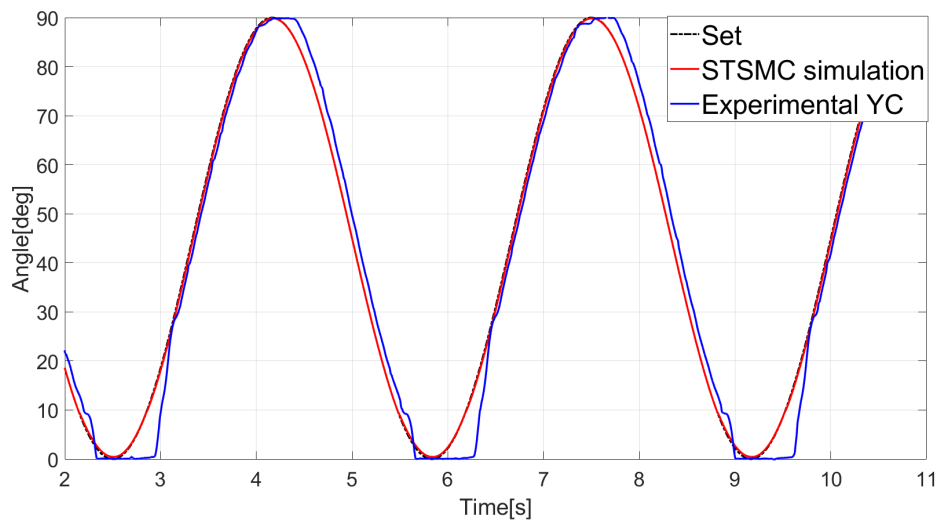


Figure 5.10: Sine Simulation Comparison

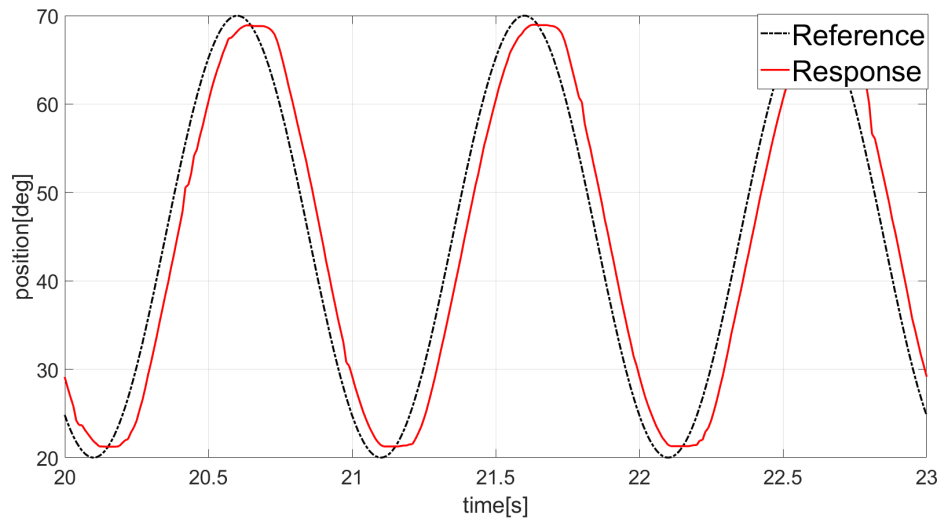


Figure 5.11: Sine Simulation at 1Hz (Youla-Coucera)

Chapter 6

Conclusions

The thesis aim is to find the most performing and most suitable type of controller for an eventual universal controller that serve the purpose of testing different types of Electronic Throttle Valve.

After a theoretical presentation and a comparison between the characteristics of the different controller architectures , with the help of simulations it is possible to determine the one with the best performances compliant with the final object of the elaborate.

The two main controller technologies taken in exam are the Sliding Mode control and Super Twisting Sliding Mode control. This choice is done considering the previous work done for the company that was based on a Youla-Coucera parametrized controller with feed forward compensation of nonlinearities. Although the performances were good for a majority of angle set signals, it lacked in robustness near the limp home position(rest position) of the ETV , where the nonlinearity terms are stronger, and so for small angles the tracking was not ensured.

SMC and STSMC are nonlinear control techniques, so they directly consider the nonlinearities of the system in the formulation of the problem, so the robustness issue are solved. However the first solution with SMC presented a problem called 'chattering' that are oscillations near the sliding surface caused by the discontinuous term of the controller, furthermore its formulation still presents dependencies from the ETV parameters.

The STSMC is an improvement of the classical SMC that reduce chattering phenomenon. This feature is achieved by means of the higher order sliding modes that allow to have a smooth control action. This formulation have also the peculiarity of being independent from the system parameters.

Analyzing the simulation done for the Sliding Mode controllers it turned out that the performances of the STSMC are the best in terms of rising time and in terms of non-linearity compensations , as the tracking for small angles resulted to be stable. In addition, the STSMC, lands itself for an easy tuning that does not depend on

the valve parameter directly , so making it the perfect choice for a self tuning scenario.

6.1 Future works

Considering the work done during this project some consideration can be done about improvements and future works:

- Up to now the validation and testing of the controller models has been carried out in the Simulink[®] environment and the results has been compared with the experimental data of the previous work done in collaboration with the company. A first step forward it is surely to build a valid controller scheme in the labVIEW environment, that is the software used for interfacing with the actual testbench. Some validation can be done in this phase before doing the actual experimental analysis on the real simulation environment.
- As mentioned in the previous point, in order to have a system that is able to work in real applications it is necessary to use measurement instruments that put our developed controller in real working context. This inevitably leads to translate the system in software and run assessments on the tesbench to certify the robustness in the real harness.
- Moreover, an open point still remain regarding the generalization of control system and his total independence from the different valve parameters. This is an important topic for the company because this kind of solution will significantly increase the efficiency of testing procedure by reducing the time needed for the retuning. It has been seen in this work that the Super Twisting Sliding Mode Control technique lands itself to be used for the purpose since his formulation depends only on the bounds of some parameters and not directly on them. A straightforward solution to this problem can be found in [6] , where the parameters of an Higher Order Sliding Mode Controller are estimated on-line by means of a Genetic Algorithm.

Appendix A

MATLAB code

A.1 Sliding Mode Controller nonlinear term evaluation

```
1
2 %% Nonlinear
3 Ks = ((K_s_pos-K_s_neg)/2)*tanh(coeff*(x1 - phi_0)) + ((K_s_pos+
   K_s_neg)/2);
4 Tpl = ((T_pl_pos-T_pl_neg)/2)*tanh(coeff*(x1 - phi_0)) + ((T_pl_pos+
   T_pl_neg)/2);
5 Tc = ((T_c_pos-T_c_neg)/2)*tanh(coeff*(x1 - phi_0)) + ((T_c_pos+
   T_c_neg)/2);
```

A.2 Sliding Mode Controller implementation

```
1 %% SM paramers
2 k1 = 400;
3 k2 = 50;
4 eta = 10;
5
6 eps = x1 - xs;
7 g = (1/I_1)*k_t*ratio/R_a;
8
9 f = (1/I_1)*(-(k_e*k_t/R_a)*x2*ratio^2 - ...
10      (T_m + B_m*x2*ratio + C_Dm*x2^2*ratio^2)*(x2)*ratio^2 - B_l*
   x2 - Ks*(x1 - phi_0) - Tpl - Tc*sign(x2));
11 %% sliding manifold
```

```
12
13 s = x2 - xs_d + k2*eps;
14
15 %% control law
16 u = -(1/g)*( -f + xs_dd - k2*(x2-xs_d) ) -k1*tanh(eta*s);
17
18
19 end
```

A.3 Super Twisting SMC implementation

```
1 %% SM paramers
2 lambda = 1;
3 k2 = 10;
4 alpha = 1;
5
6 eps = x1 - xd;
7
8 %% sliding manifold
9
10 s = x2 - xdd + k2*eps;
11
12 %% control law
13 u = -lambda*abs(s)^0.5*sign(s) + nu;
14 nu_d = -alpha*sign(s);
15
16
17 end
```

Appendix B

labVIEW code

```
1 %% Parameters
2 tau = 59^2/100;
3 eta = 1;
4 phi_0 = 9,54;
5
6 T_c_pos = 0.01999;
7 T_c_neg = 0.072206;
8 T_pl_pos = 0.23889;
9 T_pl_neg = -0.32338;
10
11 T_m = 0.0022759;
12
13 K_s_neg = 0.64785; %Spring stiffness (N*m/rad) (phi<phi_0)
14 K_s_pos = 0.074151;
15 B_l = 0.014242;
16 B_m = 1.1728e-6;
17
18 pi=4*atan(1);
19 sign_vel
20 phi
21 wm = tau*phi_dot/180*pi;
22 %% Calculation
23 phi_dot
24 T_visc = (B_l/(tau*eta)+B_m)*wm;
25 if phi<phi_0
26     delta = -((T_pl_neg-T_pl_pos)+(K_s_neg-K_s_pos)*(phi-phi_0)/180*pi)/(tau
27     T_coulomb = (T_c_pos/(tau*eta)+T_m)*sign_vel;
28 else
29     delta = -(T_pl_pos/(tau*eta)+K_s_pos*(phi-phi_0)/180*pi/(tau*eta));
30     T_coulomb = (T_c_neg/(tau*eta)+T_m)*sign_vel;
31 end
32
33 T = T_coulomb + delta+T_visc;
34
35
```

Figure B.1: Evaluation of nonlinear actions in labVIEW

Acronyms

ETV

Electronic throttle valve

SMC

Sliding Mode control

STSMC

Super Twisting Sliding Mode control

VSS

Variable Structure System

HOSM

Higher Order Sliding Mode

TA

Twisting Algorithm

ECU

Electronic Control Unit

EMF

Electro Motive Force

YC

Youla-Coucera

Bibliography

- [1] RHEINMETALL - THECNIPedia. *Throttle valves and regulating throttles*. <https://www.ms-motorservice.com/en/technipedia/post/throttle-valves-and-regulating-throttles/>. Online; accessed 4 April 2023. 2023 (cit. on p. 1).
- [2] Wikipedia. *Throttle*. <https://en.wikipedia.org/wiki/Throttle>. Online; accessed 4 April 2023. 2023 (cit. on p. 1).
- [3] Shibly A. Al-Samarraie and Yasir Abbas. «Design of Electronic Throttle Valve Position Control System using Nonlinear PID Controller». In: *International Journal of Computer Applications* 59 (2012), pp. 27–34 (cit. on p. 2).
- [4] Parrinello Niosi. ita. In: *CARATTERIZZAZIONE ELETTROMECCANICA E FLUIDODINAMICA DI UN CORPO FARFALLATO*. Marine Offshore Renewable Energy Lab (MOREnergy Lab) Politecnico di Torino, Turin, Italy, 2022 (cit. on pp. 3, 5, 7, 11, 13).
- [5] Carlo Rossi, Andrea Tilli, and A. Tonielli. «Robust control of a throttle body for drive by wire opening of automotive engines». In: *Control Systems Technology, IEEE Transactions on* 8 (Dec. 2000), pp. 993–1002. DOI: 10.1109/87.880604 (cit. on p. 3).
- [6] Mao Ye and Hai Wang. «A Robust Adaptive Chattering-Free Sliding Mode Control Strategy for Automotive Electronic Throttle System via Genetic Algorithm». In: *IEEE Access* 8 (2020), pp. 68–80. DOI: 10.1109/ACCESS.2019.2934232 (cit. on pp. 4, 43).
- [7] Mingguang Dai, Rong Qi, and Xi Cheng. «Super-Twisting Sliding Mode Control Design for Electric Dynamic Load Simulator». eng. In: *2019 Chinese Control Conference (CCC)*. Vol. 2019-. Technical Committee on Control Theory, Chinese Association of Automation, 2019, pp. 3078–3083. ISBN: 9789881563972 (cit. on pp. 4, 21).

- [8] Amjad J. Humaidi and Akram H. Hameed. «Design and Comparative Study of Advanced Adaptive Control Schemes for Position Control of Electronic Throttle Valve». In: *Information* 10.2 (2019). ISSN: 2078-2489. DOI: 10.3390/info10020065. URL: <https://www.mdpi.com/2078-2489/10/2/65> (cit. on p. 5).
- [9] University of Washington. *Inversion based feedforward theory*. https://faculty.washington.edu/devasia/Talks/Inversion_Theory.pdf. Online; accessed 27 April 2023. 2023 (cit. on p. 14).
- [10] V. Utkin. «Variable structure systems with sliding modes». In: *IEEE Transactions on Automatic Control* 22.2 (1977), pp. 212–222. DOI: 10.1109/TAC.1977.1101446 (cit. on p. 16).
- [11] Andrzej Bartoszewicz and Justyna Żuk. «Sliding mode control — Basic concepts and current trends». In: *2010 IEEE International Symposium on Industrial Electronics*. 2010, pp. 3772–3777. DOI: 10.1109/ISIE.2010.5637990 (cit. on pp. 16, 20).
- [12] Wilfrid Perruquetti and Jean Pierre Barbot. *Sliding Mode Control In Engineering*. MARCEL DEKKER, INC., 2002 (cit. on pp. 20, 21).
- [13] Sohom Chakbarty. *Sliding Mode Control and Observation - Lecture notes*. Indian Institute Of Technology - Roorkee, 2022 (cit. on p. 21).
- [14] Yuri B. Shtessel, Jaime A. Moreno, and Leonid M. Fridman. «Twisting sliding mode control with adaptation: Lyapunov design, methodology and application». In: *Automatica* 75 (2017), pp. 229–235. ISSN: 0005-1098. DOI: <https://doi.org/10.1016/j.automatica.2016.09.004>. URL: <https://www.sciencedirect.com/science/article/pii/S0005109816303399> (cit. on p. 21).